The performance of cross-linked acellular arterial scaffolds as vascular grafts; pre-clinical testing in direct and isolation loop circulatory models

Dr Timothy Pennel

Supervisor: Assoc. Prof Deon Bezuidenhout

Co-Supervisor: Prof Peter Zilla

Presented for the Degree of MMED Cardiothoracic Surgery

Chris Barnard Division of Cardiothoracic Surgery

Department of Surgery

Faculty of Health Sciences

University of Cape Town

February 2016

Declaration

I, Timothy C Pennel hereby declare that this dissertation is my own work, both in concept and execution, but for the normal guidance received from my supervisor and contributions from others as outlined in the acknowledgements. Neither the substance nor any part of this thesis has been, is being submitted or is to be submitted for another degree at this university or at any other university.

I grant the University of Cape Town free license to reproduce this thesis in print format in whole, or in part, for the purpose of research.

This thesis is presented for examination for the degree of MMED.

Signed by candidate

Signed

22/5/2016

Dated

Abstract

There is a significant need for small diameter vascular grafts to be used in peripheral vascular surgery; however autologous grafts are not always available, synthetic grafts perform poorly and allografts and xenografts degenerate, dilate and calcify after implantation. We hypothesized that chemical stabilization of acellular xenogenic arteries would generate off-the-shelf grafts resistant to thrombosis, dilatation and calcification. To test this hypothesis, we decellularized porcine renal arteries, stabilized elastin with penta-galloyl glucose and collagen with carbodiimide/activated heparin and implanted them as transposition grafts in the abdominal aorta of rats as direct implants and separately as indirect, isolation-loop implants. All implants resulted in high patency and animal survival rates, ubiquitous encapsulation within a vascularized collagenous capsule, and exhibited lack of lumen thrombogenicity and no graft wall calcification. Peri-anastomotic neo-intimal tissue overgrowth was a normal occurrence in direct implants; however this reaction was circumvented in indirect implants. Notably, implantation of nontreated control scaffolds exhibited marked graft dilatation and elastin degeneration; however, PGG significantly reduced elastin degradation and prevented aneurismal dilatation of vascular grafts. Overall these results point to the outstanding potential of crosslinked arterial scaffolds as small diameter vascular grafts.

Acknowledgements

The completion of this dissertation would not have been possible without the support of the Chris Barnard Division of Cardiothoracic Surgery. I greatly appreciate the Division's recognition of the importance of laboratory based research. I would like to specifically acknowledge the support I have received for the following people:

To my supervisor Assoc. Prof. Deon Bezuidenhout, head of biomaterials at the Cardiovascular Research Unit, and co-supervisor and Professor Peter Zilla, Head of the Chris Barnard Division of Cardiothoracic Surgery. Thank you for creating opportunities by providing an environment that is conducive to research and a centre of excellence that allows for scientific pursuit. Most importantly, I appreciate the enthusiasm you have shared with me as well as the time you have spent to council and motivate me when I have lost direction. I feel very privileged to have worked under such and influential and inspiring leaders in my short career as a cardiothoracic surgeon and researcher.

Thank you to Professor Dan Simionsecu, Head of Department Biocompatibility and Tissue Regeneration Laboratories, Department of Bioengineering, Clemson University, Clemson, SC, USA for the major contributions you have made in the concept, design, funding and implementation of study. To Dr George Fercana, Clemson University for the preparation and decellularization of the porcine renal artery, as well as pre-implant bench data.

I wish to thank my best friend, wife and part time statistical advisor Kathryn for the constant support you have shown.

Funding
NIH Fogarty International Research Collaboration Research Award (FIRCA, R03 TW008941) to Dan Simionescu.

Table of Contents

List of Tables and figures

Section I

Literature Review

1. Introduction

The treatment of symptomatic peripheral arterial disease (PAD) centres around the surgical revascularisation of ischaemic tissue. Although minimally-invasive techniques provide an attractive solution, open surgical bypass of the occluded vessel is the gold standard for achieving reperfusion[1], [2]. Despite six decades of research focussing on the development of a synthetic alternative, autologous tissue remains the conduit of choice for this procedure[3]. Both arterial (internal mammary, radial and gastro-epiploic artery) and venous (saphenous and basilic) grafts are used in cardiovascular applications, with veins being the conduit of choice in PAD[1], [2]. The advantages of autologous implants include their resistance to infection as well as long term patency, but their use is limited by availability and harvest morbidity, prompting the search for synthetic option.

Contemporary synthetic materials perform adequately in medium to large diameter vessels (≥6mm), but the use of a satisfactory small-diameter conduit remains inappropriate due to acute thrombotic occlusion and chronic anastomotic overgrowth in the form of intimal hyperplasia[4]. Initial research in vascular grafts focused on developing non-reactive substances to limit the host response. More recently, the goal has shifted to integrating biological materials within the circulatory system through tissue engineering[5]. This form of regenerative medicine integrates both absorbable as well as non-degenerating materials to organise cells in a coherent arrangement within a scaffold[6]. The degree of tissue engineering can range from a single layer of cells to the high complexity of a solid organ[7]. Despite advances in other organ systems, a clinically applicable tissue engineered blood vessel does not yet exist.

The concept of decellularization aims to separate all cellular material and antigenic debris from the donor vessel extracellular matrix (ECM) to create an inert tube that also functions as a scaffold for tissue ingrowth[8]. This process simplifies the tissue engineering requirements by providing a pre-existing construct for host cellular ingrowth. Ultimately, the objective is to develop a vascular graft from a decellularized xenogeneic tissue for treatment of small vessel occlusion.

2. Peripheral arterial disease

PAD is a diffuse atherosclerotic arteriopathy that is a clinical manifestation of chronic arterial occlusion defined by a pulse pressure differential between the upper and lower limb[9], [10]. This progressive vascular disorder is initiated by high plasma concentrations of low-density lipoprotein, which incite an inflammatory process resulting in vessel occlusion[11], [12]. PAD is associated with significant morbidity, but peripheral arterial occlusion does not itself result in death. However, it is a marker of systemic atherosclerosis and is associated with coronary artery disease and myocardial infarction[13]. Therefore, the management should involve a holistic approach that addresses risk modification and secondary prevention. The treatment of hyperlipidaemia, diabetes mellitus and hypertension as well as ensuring smoking cessation and the implementation of anti-platelet therapy, are fundamental to prevent atherosclerotic progression[1], [2]. Limb specific management focuses on revascularisation for symptom relief from vascular insufficiency ulcers as well as pain in the form of claudication. More importantly the goal is to prevent loss of the diseased limb, which has a five yearly risk of 1.0-3.3% [14].

A third of the 27 million patients in the USA diagnosed with PAD are symptomatic requiring some form of medical intervention[15], [16]. Although the full extent of atherosclerotic disease in Sub-Saharan Africa is not yet defined, a recent increase in the incidence has had a significant impact on the heath system[17]. Similarly, the incidence in South Africa is estimated to be in line with global reporting based on small observational studies[16], [18].

The management of symptomatic PAD is dependent on the revascularisation of ischaemic tissue through arterial bypass[1], [2]. The femoropopliteal segment is the most commonly treated infra-inguinal artery, and open bypass with autologous saphenous vein is the standard of care with best patency and limb salvage rates. However, autologous tissue is unavailable up to 40% of the time, requiring a synthetic alternative[19]. Despite less than satisfactory results for current synthetic implants (40% patency at 5 years) there is no superior alternative[20]. Although endovascular approaches have also been applied for PAD, stenting

remains controversial in distal disease despite the established indication in more proximal aortoiliac disease. Thus the challenge remains since contemporary designs remain inadequate for small diameter vessel reconstruction.

3. Contemporary Vascular Grafts

In the absence of autologous material, synthetics have been implanted as an arterial substitute for vascular reconstruction. There are currently two widely used materials as vascular conduits: Polyethylene terephthalate (PET) and Polytetrafluoroethylene (PTFE), which have created separate niches within vascular surgery in the absence of evidence to support their differential use[21], [22].

The combination of ethylene glycol and terephthalic acid form a thermoplastic resin known as PET (Terylene®, Dacron®)[23], [24]. PET vascular grafts are constructed as a textile tube in a woven or knitted form as a multifilament yarn that has a tensile strength of 170 MPa and modulus of 14 000MPa[25]. The conduit can be further supported by spirals or crimped to improve radial strength and kink-resistance. Despite the concern that knitted PET has a tendency to dilate under arterial pressure, few clinical complications have been reported and no clinical difference has been demonstrated between the knitted or woven designs[21], [26]. The textile nature of PET allows for bifurcating grafts and large diameter constructions and by further adding velour techniques, tissue ingrowth can be optimised. As a result PET has become the conduit of choice for medium to large diameter grafts[27].

PTFE (Gore-Tex®, Teflon®) is a inert fluorocarbon that can be expanded in to a porous form known as ePTFE[4], [26]. It is moderately stiff (100 MPa) with a lower tensile strength than that of PET (14MPa)[25], but highly flexible and permeable to gases. PTFE was initially trialled as a textile, but has been exclusively implanted as ePTFE since 1972[28]. Porosity is determined but the internodal distance (distance between the solid nodes created in the extrusion process), where distances less than 30μm are referred to as low porosity and those greater than 45μm as high porosity graft. The majority of clinical implanted ePTFE grafts

are marketed as 30μm IND and the graft is predominantly used in medium to small vessel positions.

Although these synthetic grafts have been used successfully in large calibre arteries with an acceptable long-term outcome, the intrinsic thrombogenicity of these materials and compliance mismatch leads to poor short and long term outcome in small to medium vessels. Short term results of biological grafts have been promising but have failed beyond one year due to calcification and aneurysmal dilatation. The challenge remains to develop biological grafts that maintain long term patency through optimisation of graft properties.

4. Properties of vascular grafts

Vascular graft development aims to maintain a stable conduit with long term patency[29]. However, this goal has been referred to as a 'holy grail' due to the inherent complexities of integrating synthetic material in a dynamic circulatory system[30]. Inappropriate patient selection, surgical technique[31] and calibre mismatch[32] may contribute to graft failure, but the multifaceted interaction between host vessel and the graft accounts for the majority of vessel occlusion.

Graft design has to allow for the physical demands (burst pressure, compliance and suture retention) as well as biocompatibility of all surface interactions when implanted in the circulation. This strength of a conduit is defined by the 'burst pressure', which is measured by exposing the graft to increasing hydrostatic forces[33]. The moment where the closed system measures a sharp drop in pressure, represents mural compromise and graft failure. Carotid arteries and saphenous veins have a burst pressure of 5000mmHg and 2250mmHg respectively, but 300-500mmHg is regarded as the minimum requirement for a synthetic arterial implant[34]. Since wall tension is proportional to the diameter and wall thickness of a cylinder (law of La Place), small diameter grafts require significantly higher pressures to exert the same amount of force. As a result, burst pressures are seldom a limiting factor in grafts less than six millimetres in diameter. Mural weakness resulting in aneurysmal dilatation of small diameter grafts is however a well documented phenomenon and the aetiology is multifactorial. In bioprosthetic implants the degradation of elastin and collagen by matrix

metalloproteinases (MMPs) initiate mural weakening and dilatation. Synthetic grafts are largely resistant to degradation, unless specifically designed to do so as in the case of degradable polymers. However, aneurysmal dilatation may still occur due to inherent structural design flaws, such as in knitted textiles[26] and unwrapped ePTFE grafts[35]. This is of particular concern since aneurysmal dilatation leads to an exponential rise in wall tension, increasing the risk of graft rupture.

Compliance of a vessel or conduit is defined by the change in diameter between systolic and diastolic pressure[36]. An artery is usually exposed to a pulse pressure variation of 40mmHg with 10-15% compliance. Although blood vessels have non-linear elastic properties and stiffen with increasing pressures, their maximal compliance is within the physiological blood pressure range and is significantly higher than contemporary synthetic grafts[25]. This interaction between the native vessel and implanted conduit results in a compliance mismatch with anastomotic flow disturbance. This turbulent flow results in endothelial cell damage that triggers tissue remodelling and ultimately intimal hyperplasia[36], [37]. Thus an aim of conduit development would be to construct a graft with a compliance profile that matches the host artery to limit perianastomotic hyperplasia.

Suture retention strength has been documented as an important feature of a vascular graft design. It is a logical prerequisite as sutures are required to anastomose the graft in position, but as yet, no literature has determined the ideal or adequate conditions required for an implant[38]. Current literature describes suture retention forces by measuring the force required to avulse the experimental material[39], [40]. However, the authors seldom mention the calibre of the suture or alternatively reference a suture which is too large for clinically applicable anastomosis. As a result the literature predominantly reports on bench *in vitro* studies, which lack reproducibly, and seldom report specific suture strength requirements.

When one refers to biocompatibility, it is clear that the graft should be resistant to infection, non-toxic, non-allergic and not induce malignancies[4], [39], [40]. However, acute occlusion due to thrombosis has been the primary focus of graft modification. It is well established that all foreign materials in the circulatory system

are inherently thrombogenic and induce the coagulation cascade following the blood-surface interaction[41]. Thrombogenicity can in part be manipulated by altering the graft surface with biologically active compounds. The most successful treatment thus far has been heparin modification though covalent surface bonding to ePTFE grafts[42], [43], and is well established in the manufacture of cardiopulmonary bypass circuits. The manipulation of the surface with nitric oxide (NO) modification has also shown potential advances in the prevention of thrombosis as well as the down regulation of endothelial adhesion molecules and inhibition of smooth muscle proliferation[44]. Although the alteration of graft host interaction with compounds such as NO have theoretical advantages, they are currently impractical due to the finite reservoir[45], and potential carcinogenic nitrosamine formation[46].

In summary the lack of progress in synthetic vascular graft development over the last 60 years has resulted in specific modifications attempting to address isolated aspects of graft failure. However, the physical and biological attributes mentioned above are often intertwined and interdependent. As a result, the focus may require a shift away from contemporary graft modifications and optimisation towards novel biosynthetic designs.

5. Experimental solutions

Experimental graft designs have predominantly focused on two concepts; degradable synthetic polymer scaffolds and tissues engineering.

a) Degradable polymers

The design objective of total polymer resorption aims to avoid the persistent foreign body reaction seen in all non-degradable counterparts. The synthetic materials are referred to as biodegradable when enzymatically degraded or bioabsorbable when non-enzymatic chemicals breakdown the polymer. The challenge in design is to limit graft fragmentation and embolization of the degraded polymer whilst maintaining sufficient strength through tissue ingrowth before the degradation process results in graft failure[21], [47].

Polyglycolic acid (PGA) was the first degradable synthetic suture material, but due to is rapid loss of strength, could not be used for vascular graft applications[48]. PGA was subsequently methylated to form a more hydrophilic compound known as polylactic acid (PLA) and the first fully bioresorbable vascular graft was constructed out of a PGA-PLA copolymer known and polyglatin (Vicryl-PG910) [49]. Despite the initial enthusiasm with polyglactin, as with previous degradable polymer grafts it is also prone to aneurysmal dilatation and rupture. Other materials which are used clinically as sutures (polyhydroxyalkanoate, polycaprolactone and polydioxanone) have not progressed beyond clinical trials as vascular conduits despite histological evidence of intermediate stability[6].

b) Tissue Engineering

First attempts of tissue engineering involved endothelial cell transplant onto the luminal surface of permanent scaffolds to create a 'natural' barrier between the blood and synthetic material[50]. This process requires harvesting of autologous endothelial cells, which are applied to the polymeric surface immediately before implant as a single stage process, or alternatively as a two stage procedure following cell culture. Despite trial evidence of infra-inguinal patency equivalent to that of autologous veins in two -stage seeded ePTFE[51], the extreme cost and high level of expertise required to implement this technique has limited its clinical application. These constraints have not deterred researchers who continue to explore scaffold free, complete tissue engineering of the vessel, an even more complex form of tissue engineering.

More recently the concept of completely tissue engineered blood vessels (TEBV) has been proposed as a surrogate for autologous tissue[52], [53]. Their ability to remodel and repair as an autologous graft would do without a foreign body response has renewed enthusiasm as a viable alternative despite its rigorous demands. The concept relies on *ex vivo* cell culture to construct the vessel in a pulsatile bioreactor using a degradable material as a scaffold. Initially acellular collagen and PGA based degradable scaffolds were used, but neither of these techniques have been able to sustain systemic pressures. Recent optimisation with staged culture layers has resulted in the first clinical trial of a TEBV[54]. The process involves

dehydrated human skin fibroblasts, which are wrapped around a PTFE mandrill followed but the culture of an umbilical smooth muscle cell-wrap to form the media. Following a week long culture in a bioreactor, fibroblasts are added to create an adventitia and the surface is subsequently seeded with endothelium[55]. Despite excellent clinical patency of the TEBV, as with seeded ePTFE, these designs have not made any penetration beyond clinical trial due to extreme expense and expertise required to develop these models[56]. A more practical solution would therefore employ the concept of the human body as a bioreactor for a natural scaffold that would allow for *in vivo* tissue regeneration.

c) Decellularization

The inflammatory response and an immune mediated rejection initiated by antigenic remnants found in foreign tissue, remains an inherent challenge in cross-species implants[57]. In an attempt to replicate the performance of autologous tissue, researchers have eliminated these cellular products from xeno- and allograft tissues[58]. Unlike TEBV, this process of decellularization is a 'top-down' approach of modifying naturally occurring scaffolds rather than *de novo* construction and is thus significantly less complex or costly[33].

Following the removal of cellular material, a complex structure comprising of collagen and elastin remains that represents the ECM. This scaffold is generally non-immunogenic[59], but still provides a role for cellular migration, proliferation and differentiation[60]. The process of decellularization uses a combination of physical and chemical treatments to eliminate all cellular and nuclear materials from the tissue, with the minimal possible disturbance of mechanical integrity. Physical methods include freeze-thawing or direct pressure lysis to destabilise cellular membranes, which are often precursors to further chemical treatment. Other methods such as mechanical agitation and sonication are used simultaneously with chemical treatments to assist cell lysis and removal of debris.

A vast array of chemical treatments have been applied in the degradation of cellular materials and their utilisation is dependent on tissue characteristics as well as clinical application[60]: These range from

detergent based treatments (pH manipulation, non-ionic, ionic and zwitterionic detergents), Osmotic shock treatments (hypo- and hypertonic) as well as chelating agents. Enzymatic methods and protease inhibitors although not strictly speaking chemical treatments, are often grouped to together with the other 'non-physical' treatments. It is essential to ensure that the tissue has been adequately decellularized and verification can be performed with standard histological staining (haematoxylin and Eosin and Masson's trichrome stains) and specific immunohistochemical methods, which stain for intracellular proteins. DNA staining with DAPI is a standard method for verifying the absence of nucleic acids.

Although the ECM is responsible for maintaining structural strength, any process that involves the removal of cells will ultimately reshape the three-dimensional structure of the ECM and potentially compromise stability. As a result untreated scaffolds tend to degenerate rapidly after implantation if they are not adequately stabilised[61]. Gluteraldehyde has been widely used as a tissue fixative to stabilise, sterilise and reduce antigenicity of tissue[62]. The di-aldehyde bonds of gluteraldehyde react with the free amine groups on the ECM, more specifically collagen, and cross-link to strengthen the tissue. Although collagen cross-linking adds strength, the tissue is more prone to calcification following gluteraldehyde fixation and since elastin devoid of amine groups, it remains untreated allowing for enzymatic degradation of this important molecule. It is clear that current tissue fixation techniques require optimisation. Novel research with tannic acids such as pentagalloyl glucose(PGG) have been shown to specifically bind to elation and render it resistant to the enzymatic degradation and aneurysm formation[63].

Pre-clinical and human applications of decellularized tissues have already been implanted in other positions[58], [64], [65], but have yet to be successfully implemented as vascular conduits. It is clear that researchers need to employ decellularization techniques that limit the damage to the ECM integrity whilst ensuring the removal of all antigenic material. Novel stabilisation techniques the preserve the function of both elastin and collagen are essential for long-term patency and structural integrity.

6. *In vivo* model designs

Novel conduit development has relied on *in vivo* animal implants to clarify compatibility and identify graft-host interactions[66]. Not only are pre-clinical implants a requirement for regulatory approval prior to a clinical trial, the *in vivo* simulation provides researchers with information that would not be available through *ex vivo* bench testing. It is however essential to select an animal model that provides the appropriate anatomy, physiology and pathological environment for human extrapolation and implementation. It is clear that the primate would be the logical choice if only to fulfil the above requirements, but the ethics and financial implications of primate based research has largely rendered this model obsolete. As a result, other large animal models (ovine, porcine and canine) dominate the literature, but even these have significant cost implications if not implemented appropriately. The high-throughput, cost effective small animal model has been widely used as a screening tool, preceding the large animal implant.

The rat is widely established as a circulatory model with many similarities to the haemodynamic profile of humans. A blood pressure of 127±7mmHg (systolic) and 85±2mmHg (diastolic) is ideal to simulate a human implant and the 'supra-normal' heart rate of 250 to 450bmp exposes the graft to four times the cycles that a human graft would endure over the same time period[66]. An 18 month rat experiment is considered the entire lifespan of the animal with accelerated aging compared to a human[67]. It is postulated that the rapid metabolic turnover would represent a long-term implant in a human although the exact haemodynamic consequences of this high heart rate can only be extrapolated from other haemodynamic data.

Haemodynamic factors, such as: flow (mL/min), velocity (cm/s) and wall shear stress (dynes/cm^2) have an effect on conduit and cellular function. Although there appears to be a direct linear correlation between blood-flow and animal size, the velocity of blood remains static with respect to species[66]. A second factor is the variation in flow between arterial sites, within the same species. For example, there is a direct relationship between carotid artery flow and body mass, which is not observed in the femoral artery.[68] However, these data are heterogeneous and dependent on the method of measurement as well loading

conditions during anaesthesia [69].

Although also subject to the same variability, wall shear stress has significant effect on vascular graft healing and endothelial adhesion molecules[70] as the tangential component of frictional forces generated at the vessel surface have been shown to affect healing and cellular interaction[68]. The endothelium endure most of the wall shear stress and recent studies have shown that flow disturbances are responsible for atherogenesis and plaque formation[71] The magnitude of shear stress is directly proportional to the viscosity of blood, which remains relatively constant across species, but is inversely proportional to the radius of the vessels. It is for this reason that shear stress is directly proportional to species size. Human arteries have a shear stress of 10 to 70 dyn/cm^2 [71], [72], whereas the shear stress in the rodent aorta is tenfold higher with measurements up to 600dyn/cm^2 [73]. This significantly higher shear stress would have implications not only for the ability of endothelium to remain attached to the surface of a synthetic conduit, but would also limit the adhesion of platelets further reducing the thrombogenicity of the implanted foreign material. Observations have however shown that vascular remodelling is dependent on the change in shear stress rather than the absolute value[74], [75], and thus the impact of this interspecies variability remains speculative.

Furthermore, the rat has a significantly less demanding coagulation cascade than other mammals which results in significantly higher patency. Although this may be of benefit for assessing prototype graft designs, investigators are often frustrated by poor graft performance when implanted in larger animals. It is for this reason that rats should not be used for thrombogenic models but for evaluating physical properties and healing. Further consideration has to be given to the age of the animal, with particular reference to the intended implant age of the index human patient. PAD predominantly affects senescent individuals, which would impact on the regenerative potential in clinical practise. Synthetic graft healing has been shown to be less effective in older animals, which is likely to be mirrored in the clinical implant into aged human patients. This data is however not linear and interpretation is complex due to the heterogeniticy of techniques used to measure healing[76]. This further complicated by cross-species variation, with juvenile baboons displaying

similar healing characteristics to senescent dogs[29]. It is clear that every animal model has limitations, which should be carefully considered when interpreting the data. The challenge therefore is to choose the appropriate model to answer the research question posed and ensure that it is fully optimised to deliver the appropriate result.

Few animal models employ representative graft lengths and this is of particular relevance in the rat. A mean length of 18.1±26.6mm [2-100mm) is reported in the literature. As a result 90% of grafts are too short to have clinical relevance in PAD[29]. The 10% that are of adequate length are looped within the abdomen to increase the length of the infra-renal segment[77]. But even lengths of 10cm are too short to adequately simulate clinically implanted graft for PAD, which are as long as 40cm[29]. It is however possible to simulate mid-graft healing by isolating it from the anastomosis allowing for independent analysis. Mid-graft isolation models have been implemented successfully in large animal model[78], but the recent application of a looped isolation model in the rat has allowed for high throughout endothelial analysis[79].

The combination of looping an infra-renal graft and isolating it from the anastomosis allows the research to independently assess transanastomotic as well and mid-graft healing of the experimental model. By implementing this philosophy in a small animal model such as a rat one is able to inexpensively asses healing in a high throughput model.

7. Summary

PAD is a global pandemic with an increasing incidence in the developing world. Despite efforts to limit the progression of the disease through primary and secondary prevention, symptomatic patients still require open surgical bypass for pain relief and limb salvage. Vascular graft research has stagnated over the last sixty years with little alternative to autologous vein bypass of the occluded peripheral artery. Despite a renewed focus on tissue engineering with promising results from TEBV, the translation from the laboratory to the clinic remains elusive. A simplified concept of tissue engineering where the pre-existing ECM construct is isolated

through decellularization appears to be a logical solution to this complex obstacle. More importantly *in vivo* models need to be designed to analyse both anastomotic interaction as well as mid-graft healing and the implementation of isolated mid-segments are essential in high throughput rodent models. It is with the combination of a simplified tissue engineering concept together with an appropriate model design that will potentially solve the current challenge that faces vascular graft developers.

8. References

[1] M. Tendera, V. Aboyans, M.-L. Bartelink, I. Baumgartner, D. Clément, J.-P. Collet, A. Cremonesi, M. De Carlo, R. Erbel, F. G. R. Fowkes, M. Heras, S. Kownator, E. Minar, J. Ostergren, D. Poldermans, V. Riambau, M. Roffi, J. Röther, H. Sievert, M. van Sambeek, T. Zeller, ESC Committee for Practice Guidelines, P. Kolh, and A. Torbicki, "ESC Guidelines on the diagnosis and treatment of peripheral artery diseases: Document covering atherosclerotic disease of extracranial carotid and vertebral, mesenteric, renal, upper and lower extremity arteries: the Task Force on the Diagnosis and Treatment of Peripheral Artery Diseases of the European Society of Cardiology (ESC).," *European Heart Journal*, vol. 32, no. 22. pp. 2851–2906, Nov-2011.

[2] T. W. Rooke, A. T. Hirsch, S. Misra, A. N. Sidawy, J. A. Beckman, L. K. Findeiss, J. Golzarian, H. L. Gornik, J. L. Halperin, M. R. Jaff, G. L. Moneta, J. W. Olin, J. C. Stanley, C. J. White, J. V. White, R. E. Zierler, and A. K. Jacobs, "2011 ACCF/AHA Focused Update of the Guideline for the Management of Patients With Peripheral Artery Disease (Updating the 2005 Guideline): A Report of the American College of Cardiology Foundation/American Heart Association Task Force on Practice Guidelines," *Circulation*, vol. 124, no. 18, pp. 2020–2045, Oct. 2011.

[3] M. A. Twine CP, "Graft type for femoro-popliteal bypass surgery (Review)," pp. 1–89, Jan. 2013.

[4] J. Chlupáč, E. Filova, and L. Bačáková, "Blood vessel replacement: 50 years of development and tissue engineering paradigms in vascular surgery," *Physiol Res*, vol. 58, no. 2, pp. S119–S139, 2009.

[5] L. Ye, J. Cao, L. Chen, X. Geng, A.-Y. Zhang, L.-R. Guo, Y.-Q. Gu, and Z.-G. Feng, "The fabrication of double layer tubular vascular tissue engineering scaffold via coaxial electrospinning and its 3D cell coculture.," *J Biomed Mater Res A*, vol. 103, no. 12, pp. 3863–3871, Dec. 2015.

[6] G. R. Campbell and J. H. Campbell, "Development of tissue engineered vascular grafts.," *Curr Pharm Biotechnol*, vol. 8, no. 1, pp. 43–50, Feb. 2007.

[7] M. Birchall and G. Hamilton, "Tissue-engineered vascular replacements for children," *The Lancet*, vol. 380, no. 9838, pp. 197–198, Jul. 2012.

[8] L. Mancuso, A. Gualerzi, F. Boschetti, F. Loy, and G. Cao, "Decellularized ovine arteries as small-diameter vascular grafts," *Biomed. Mater.*, vol. 9, no. 4, pp. 045011–10, Aug. 2014.

[9] P. C. Bennett, S. H. Silverman, P. S. Gill, and G. Y. H. Lip, "Peripheral arterial disease and Virchow's triad.," *Thromb. Haemost.*, vol. 101, no. 6, pp. 1032–1040, Jun. 2009.

[10] A. Kumar, B. Mash, and G. Rupesinghe, "Peripheral arterial disease - high prevalence in rural black South Africans.," *S. Afr. Med. J.*, vol. 97, no. 4, pp. 285–288, Apr. 2007.

[11] B. Enkhmaa, K. Shiwaku, E. Anuurad, A. Nogi, K. Kitajima, M. Yamasaki, T. Oyunsuren, and Y. Yamane, "Prevalence of the metabolic syndrome using the Third Report of the National Cholesterol Educational Program Expert Panel on Detection, Evaluation, and Treatment of High Blood Cholesterol in Adults (ATP III) and the modified ATP III definitions for Japanese and Mongolians," *Clinica Chimica Acta*, vol. 352, no. 1, pp. 105–113, Feb. 2005.

[12] K. J. Moore and I. Tabas, "Macrophages in the pathogenesis of atherosclerosis.," *Cell*, vol. 145, no. 3, pp. 341–355, Apr. 2011.

[13] K. Ouriel, "Peripheral arterial disease.," *The Lancet*, vol. 358, no. 9289, pp. 1257–1264, Oct. 2001.

[14] I. Baumgartner, R. Schainfeld, and L. Graziani, "Management of Peripheral Vascular Disease," *Annu. Rev. Med.*, vol. 56, no. 1, pp. 249–272, Feb. 2005.

[15] P. Aylin, T. Lees, S. Baker, D. Prytherch, and S. Ashley, "Descriptive Study Comparing Routine Hospital Administrative Data with the Vascular Society of Great Britain and Ireland's National Vascular Database," *European Journal of Vascular and Endovascular Surgery*, vol. 33, no. 4, pp. 461–465, Apr. 2007.

[16] A. Abdool-Carrim, "CPD Article: Peripheral Arterial Disease," *South African Family Practice*, vol. 46, no. 8, 2004.

[17] K. Tibazarwa, L. Ntyintyane, K. Sliwa, T. Gerntholtz, M. Carrington, D. Wilkinson, and S. Stewart, "A time bomb of cardiovascular risk factors in South Africa: results from the Heart of Soweto Study "Heart Awareness Days".," *International Journal of Cardiology*, vol. 132, no. 2, pp. 233–239, Feb.

2009.
[18] J. V. Robbs, “Atherosclerotic peripheral arterial disease in blacks--an established problem.,” *S. Afr. Med. J.*, vol. 67, no. 20, pp. 797–801, May 1985.
[19] P. L. Faries, F. W. LoGerfo, S. Arora, M. C. Pulling, D. I. Rohan, C. M. Akbari, D. R. Campbell, G. W. Gibbons, and F. B. Pomposelli, “Arm vein conduit is superior to composite prosthetic-autogenous grafts in lower extremity revascularization.,” *YMVA*, vol. 31, no. 6, pp. 1119–1127, Jun. 2000.
[20] C. McCollum, G. Kenchington, C. Alexander, P. J. Franks, and R. M. Greenhalgh, “PTFE or HUV for femoro-popliteal bypass: A multi-centre trial,” *European Journal of Vascular Surgery*, vol. 5, no. 4, pp. 435–443, Aug. 1991.
[21] L. Xue and H. P. Greisler, “Biomaterials in the development and future of vascular grafts,” *Journal of vascular surgery*, vol. 37, no. 2, pp. 472–480, Feb. 2003.
[22] S. Roll, J. Muller-Nordhorn, T. Keil, H. Scholz, D. Eidt, W. Greiner, and S. N. Willich, “Dacron vs. PTFE as bypass materials in peripheral vascular surgery - systematic review and meta-analysis,” *BMC Surg*, vol. 8, no. 1, p. 22, 2008.
[23] R. A. Jonas, G. Ziemer, F. J. Schoen, and L. Britton, “A new sealant for knitted Dacron prostheses: minimally cross-linked gelatin,” *Journal of vascular surgery*, 1988.
[24] M. King, P. Blais, R. Guidoin, E. Prowse, M. Marcois, C. Gosselin, and H. P. Noel, “Polyethylene terephthalate (Dacron) vascular prostheses-material and fabric construction aspects,” *Biocompatibility of clinical implants materials. CRC Press, Boca Raton*, vol. 2, pp. 177–207, 1981.
[25] H. J. Salacinski, S. Goldner, A. Giudiceandrea, G. Hamilton, A. M. Seifalian, A. Edwards, and R. J. Carson, “The Mechanical Behavior of Vascular Grafts: A Review,” *Journal of Biomaterials Applications*, vol. 15, no. 3, pp. 241–278, Jan. 2001.
[26] R. Y. Kannan, H. J. Salacinski, P. E. Butler, G. Hamilton, and A. M. Seifalian, “Current status of prosthetic bypass grafts: A review,” *J. Biomed. Mater. Res.*, vol. 74, no. 1, pp. 570–581, 2005.
[27] D. Bezuidenhout and P. Zilla, “Vascular grafts,” *Encyclopedia of Biomaterials and Biomedical Engineering*, pp. 1715–1725, 2004.
[28] J. S. T. Yao and M. K. Eskandari, “Accidental discovery: The polytetrafluoroethylene graft,” *Surgery*, vol. 151, no. 1, pp. 126–128, Jan. 2012.
[29] P. Zilla, D. Bezuidenhout, and P. Human, “Prosthetic vascular grafts: Wrong models, wrong questions and no healing,” *Biomaterials*, vol. 28, no. 34, pp. 5009–5027, Dec. 2007.
[30] M. S. Conte, “The ideal small arterial substitute: a search for the Holy Grail?,” *FASEB J.*, vol. 12, no. 1, pp. 43–45, Jul. 1998.
[31] M. Belkin, M. S. Conte, M. C. Donaldson, J. A. Mannick, and A. D. Whittemore, “Preferred strategies for secondary infrainguinal bypass: lessons learned from 300 consecutive reoperations.,” *YMVA*, vol. 21, no. 2, pp. 282–93– discussion 293–5, Feb. 1995.
[32] P. E. Karayannacos, J. R. Hostetler, M. G. Bond, G. S. Kakos, R. A. Williams, J. W. Kilman, and J. S. Vasko, “Late failure in vein grafts: mediating factors in subendothelial fibromuscular hyperplasia.,” *Ann. Surg.*, vol. 187, no. 2, pp. 183–188, Feb. 1978.
[33] G. F. A. D. Simionescu, “Chapter 3: Polymeric Biomaterials for Vascular Tissue Engineering,” pp. 1–20, Apr. 2012.
[34] S. Sarkar, H. J. Salacinski, G. Hamilton, and A. M. Seifalian, “The Mechanical Properties of Infrainguinal Vascular Bypass Grafts: Their Role in Influencing Patency,” *European Journal of Vascular and Endovascular Surgery*, vol. 31, no. 6, pp. 627–636, Jun. 2006.
[35] C. D. Campbell, D. H. Brooks, M. W. Webster, R. P. Bondi, J. C. Lloyd, M. F. Hynes, and H. T. Bahnson, “Aneurysm formation in expanded polytetrafluoroethylene prostheses.,” *Surgery*, vol. 79, no. 5, pp. 491–493, May 1976.
[36] P. C. Ho, J. Melbin, and R. W. Nesto, “Scholarly review of geometry and compliance: biomechanical perspectives on vascular injury and healing.,” *ASAIO J*, vol. 48, no. 4, pp. 337–345, Jul. 2002.
[37] H. S. Bassiouny, S. White, S. Glagov, E. Choi, D. P. Giddens, and C. K. Zarins, “Anastomotic intimal hyperplasia: Mechanical injury or flow induced,” *Journal of vascular surgery*, vol. 15, no. 4, pp. 708–717, Apr. 1992.
[38] W. M. Abbott, A. Callow, W. Moore, R. Rutherford, F. Veith, and S. Weinberg, “Evaluation and performance standards for arterial prostheses,” *Journal of vascular surgery*, vol. 17, no. 4, pp. 746–756, Apr. 1993.

[39] P. Nair and N. Thottappillil, “Scaffolds in vascular regeneration: current status,” *VHRM*, vol. 11, pp. 79–13, Jan. 2015.
[40] J. Johnson, D. Ohst, T. Groehl, and S. Hetterscheidt, “Development of Novel, Bioresorbable, Small-Diameter Electrospun Vascular Grafts,” *J Tissue Sci …*, 2015.
[41] C. O. Esquivel and F. W. Blaisdell, “Why small caliber vascular grafts fail: a review of clinical and experimental experience and the significance of the interaction of blood at the interface.,” *J Surg Res*, vol. 41, no. 1, pp. 1–15, Jul. 1986.
[42] C. O. Esquivel, C. G. Björck, S. E. Bergentz, D. Bergqvist, R. Larsson, S. N. Carson, P. Dougan, and B. Nilsson, “Reduced thrombogenic characteristics of expanded polytetrafluoroethylene and polyurethane arterial grafts after heparin bonding.,” *Surgery*, vol. 95, no. 1, pp. 102–107, Jan. 1984.
[43] P. C. Begovac, R. C. Thomson, J. L. Fisher, A. Hughson, and A. Gällhagen, “Improvements in GORE-TEX® vascular graft performance by Carmeda® bioactive surface heparin immobilization,” *European Journal of Vascular and Endovascular Surgery*, vol. 25, no. 5, pp. 432–437, May 2003.
[44] J. Davignon and P. Ganz, “Role of endothelial dysfunction in atherosclerosis.,” *Circulation*, vol. 109, no. 23, pp. III27–32, Jun. 2004.
[45] M. R. Kapadia, D. A. Popowich, and M. R. Kibbe, “Modified Prosthetic Vascular Conduits,” *Circulation*, vol. 117, no. 14, pp. 1873–1882, Apr. 2008.
[46] K. A. Mowery, M. H Schoenfisch, J. E. Saavedra, L. K. Keefer, and M. E. Meyerhoff, “Preparation and characterization of hydrophobic polymeric films that are thromboresistant via nitric oxide release,” *Biomaterials*, vol. 21, no. 1, pp. 9–21, Jan. 2000.
[47] D. Shum-Tim, U. Stock, J. Hrkach, T. Shin'oka, J. Lien, M. A. Moses, A. Stamp, G. Taylor, A. M. Moran, W. Landis, R. LANGER, J. P. Vacanti, and J. E. Mayer, “Tissue engineering of autologous aorta using a new biodegradable polymer.,” *ATS*, vol. 68, no. 6, pp. 2298–304– discussion 2305, Dec. 1999.
[48] R. Lanza, R. Langer, and J. P. Vacanti, *Principles of Tissue Engineering*. Academic Press, 2011.
[49] S. Bowald, C. Busch, and I. Eriksson, “Arterial regeneration following polyglactin 910 suture mesh grafting.,” *Surgery*, vol. 86, no. 5, pp. 722–729, Nov. 1979.
[50] M. Herring, A. Gardner, and J. Glover, “A single-staged technique for seeding vascular grafts with autogenous endothelium.,” *Surgery*, vol. 84, no. 4, pp. 498–504, Oct. 1978.
[51] M. Deutsch, J. Meinhart, P. Zilla, N. Howanietz, M. Gorlitzer, A. Froeschl, A. Stuempflen, D. Bezuidenhout, and M. Grabenwoeger, “Long-term experience in autologous in vitro endothelialization of infrainguinal ePTFE grafts,” *Journal of vascular surgery*, vol. 49, no. 2, pp. 352–362, Feb. 2009.
[52] R. M. Nerem, “Tissue engineering a blood vessel substitute: the role of biomechanics.,” *Yonsei Med. J.*, vol. 41, no. 6, pp. 735–739, Dec. 2000.
[53] C. Weinberg and E. Bell, “A blood vessel model constructed from collagen and cultured vascular cells,” *Science*, vol. 231, no. 4736, pp. 397–400, Jan. 1986.
[54] T. N. McAllister, M. Maruszewski, S. A. Garrido, W. Wystrychowski, N. Dusserre, A. Marini, K. Zagalski, A. Fiorillo, H. Avila, X. Manglano, J. Antonelli, A. Kocher, M. Zembala, L. Cierpka, L. M. de la Fuente, and N. L'Heureux, “Effectiveness of haemodialysis access with an autologous tissue-engineered vascular graft: a multicentre cohort study.,” *Lancet*, vol. 373, no. 9673, pp. 1440–1446, Apr. 2009.
[55] N. L'Heureux, N. Dusserre, G. Konig, B. Victor, and P. Keire, “Human tissue-engineered blood vessels for adult arterial revascularization - Nature Medicine,” *Nature Medicine*, 2006.
[56] N. L'Heureux, N. Dusserre, A. Marini, S. Garrido, L. de la Fuente, and T. McAllister, “Technology Insight: the evolution of tissue-engineered vascular grafts—from research to clinical practice,” *Nat Clin Pract Cardiovasc Med*, vol. 4, no. 7, pp. 389–395, Jul. 2007.
[57] T. W. Gilbert, T. L. Sellaro, and S. F. Badylak, “Decellularization of tissues and organs.,” *Biomaterials*, vol. 27, no. 19, pp. 3675–3683, Jul. 2006.
[58] G. Dellgren, M. Eriksson, L. A. Brodin, and K. Rådegran, “The extended Biocor stentless aortic bioprosthesis. Early clinical experience.,” *Scand. Cardiovasc. J.*, vol. 33, no. 5, pp. 259–264, 1999.
[59] D. G. Seifu, A. Purnama, K. Mequanint, and D. Mantovani, “Small-diameter vascular tissue engineering,” *Nat Rev Cardiol*, vol. 10, no. 7, pp. 410–421, May 2013.
[60] P. M. Crapo, T. W. Gilbert, and S. F. Badylak, “An overview of tissue and whole organ decellularization processes,” *Biomaterials*, vol. 32, no. 12, pp. 3233–3243, Apr. 2011.

[61] M. E. Tedder, J. Liao, B. Weed, C. Stabler, H. Zhang, A. Simionescu, and D. T. Simionescu, “Stabilized collagen scaffolds for heart valve tissue engineering.,” *Tissue Engineering Part A*, vol. 15, no. 6, pp. 1257–1268, Jun. 2009.
[62] J. C. Isenburg, D. T. Simionescu, and N. R. Vyavahare, “Tannic acid treatment enhances biostability and reduces calcification of glutaraldehyde fixed aortic wall,” *Biomaterials*, vol. 26, no. 11, pp. 1237–1245, Apr. 2005.
[63] J. C. Isenburg, D. T. Simionescu, B. C. Starcher, and N. R. Vyavahare, “Elastin stabilization for treatment of abdominal aortic aneurysms.,” *Circulation*, vol. 115, no. 13, pp. 1729–1737, Apr. 2007.
[64] S. F. Badylak, “Xenogeneic extracellular matrix as a scaffold for tissue reconstruction.,” *Transplant Immunology*, vol. 12, no. 3, pp. 367–377, Apr. 2004.
[65] M. S. Lee, “GraftJacket augmentation of chronic Achilles tendon ruptures.,” *Orthopedics*, vol. 27, no. 1, pp. s151–3, Jan. 2004.
[66] M. J. Byrom, P. G. Bannon, G. H. White, and M. K. C. Ng, “Animal models for the assessment of novel vascular conduits,” *YMVA*, vol. 52, no. 1, pp. 176–195, Jul. 2010.
[67] S. de Valence, J.-C. Tille, D. Mugnai, W. Mrowczynski, R. Gurny, M. Möller, and B. H. Walpoth, “Long term performance of polycaprolactone vascular grafts in a rat abdominal aorta replacement model,” *Biomaterials*, vol. 33, no. 1, pp. 38–47, Jan. 2012.
[68] J.-J. Chiu and S. Chien, “Effects of disturbed flow on vascular endothelium: pathophysiological basis and clinical perspectives.,” *Physiol. Rev.*, vol. 91, no. 1, pp. 327–387, Jan. 2011.
[69] R. P. Forsyth and B. I. Hoffbrand, “Redistribution of cardiac output after sodium pentobarbital anesthesia in the monkey.,” *Am. J. Physiol.*, vol. 218, no. 1, pp. 214–217, Jan. 1970.
[70] P. F. Davies and S. C. Tripathi, “Mechanical stress mechanisms and the cell. An endothelial paradigm.,” *Circulation Research*, vol. 72, no. 2, pp. 239–245, Feb. 1993.
[71] A. M. Malek, S. L. Alper, and S. Izumo, “Hemodynamic shear stress and its role in atherosclerosis.,” *JAMA*, vol. 282, no. 21, pp. 2035–2042, Dec. 1999.
[72] R. M. Nerem, R. W. Alexander, and D. C. Chappell, “The study of the influence of flow on vascular endothelial biology,” *The American journal …*, 1998.
[73] J. Suo, D. E. Ferrara, D. Sorescu, R. E. Guldberg, W. R. Taylor, and D. P. Giddens, “Hemodynamic Shear Stresses in Mouse Aortas Implications for Atherogenesis,” *Arteriosclerosis, Thrombosis, and Vascular Biology*, vol. 27, no. 2, pp. 346–351, Feb. 2007.
[74] A. Kamiya and T. Togawa, “Adaptive regulation of wall shear stress to flow change in the canine carotid artery.,” *Am. J. Physiol.*, vol. 239, no. 1, pp. H14–21, Jul. 1980.
[75] B. L. Langille and F. O'Donnell, “Reductions in arterial diameter produced by chronic decreases in blood flow are endothelium-dependent,” *Science*, vol. 231, no. 4736, pp. 405–407, Jan. 1986.
[76] T. Pennel, “Isolation and optimising transmural endothelialization as an independent mode of spontaneous vascular graft healing,” Cape Town, 2014.
[77] P. H. Robinson, H. L. Bartels, and B. van der Lei, “Patency and healing of 10-cm long microarterial polytetrafluoroethylene prostheses in the rat abdominal aorta.,” *J Reconstr Microsurg*, vol. 5, no. 4, pp. 331–336, Oct. 1989.
[78] Q. Shi, S. Rafii, M. H.-D. Wu, E. S. Wijelath, C. Yu, A. Ishida, Y. Fujita, S. Kothari, R. Mohle, L. R. Sauvage, M. A. S. Moore, R. F. Storb, and W. P. Hammond, “Evidence for circulating bone marrow-derived endothelial cells.,” *Blood*, vol. 92, no. 2, pp. 362–367, Jul. 1998.
[79] T. Pennel, P. Zilla, and D. Bezuidenhout, “Differentiating transmural from transanastomotic prosthetic graft endothelialization through an isolation loop-graft model.,” *Journal of vascular surgery*, vol. 58, no. 4, pp. 1053–1061, Oct. 2013.
[80] K. Berger, L. R. Sauvage, A. M. Rao, and S. J. Wood, “Healing of arterial prostheses in man: its incompleteness.,” *Ann. Surg.*, vol. 175, no. 1, p. 118, 1972.

Section II

Manuscript

The performance of cross-linked acellular arterial scaffolds as vascular grafts; pre-clinical testing in direct and isolation loop circulatory Models

Timothy Pennel [a], George Fercana [b], Deon Bezuidenhout [a], Agneta Simionescu [b], Ting-Hsien Chuang [b], Peter Zilla [a], Dan Simionescu [b,*]

[a] *Christian Barnard Department of Cardiothoracic Surgery, Cardiovascular Research Unit, University of Cape Town, Faculty of Health Sciences,*
Cape Heart Center, Chris Barnard Building, Anzio Road, ZA 7925 Observatory, Cape Town, South Africa

[b] *Biocompatibility and Tissue Regeneration Laboratories, Department of Bioengineering, Clemson University, Clemson, SC, USA*

Abstract

There is a significant need for small diameter vascular grafts to be used in peripheral vascular surgery; however autologous grafts are not always available, synthetic grafts perform poorly and allografts as well as xenografts degenerate, dilate and calcify after implantation. We hypothesized that chemical stabilization of acellular xenogenic arteries would generate off-the-shelf grafts resistant to thrombosis, dilatation and calcification. To test this hypothesis, we decellularized porcine renal arteries, stabilized elastin with penta-galloyl glucose and collagen with carbodiimide/activated heparin and implanted them as transposition grafts in the abdominal aorta of rats as direct implants and separately as indirect, isolation-loop implants. All implants resulted in high patency and animal survival rates, ubiquitous encapsulation within a vascularized collagenous capsule, and exhibited lack of lumen thrombogenicity and no graft wall calcification. Peri-anastomotic neo-intimal tissue overgrowth was a normal occurrence in direct implants; however, this reaction was circumvented in indirect implants. Notably, implantation of nontreated control scaffolds exhibited marked graft dilatation and elastin degeneration; however, PGG significantly reduced elastin degradation and prevented aneurismal dilatation of vascular grafts. Overall these results point to the outstanding potential of crosslinked arterial scaffolds as small diameter vascular grafts.

Introduction

Almost 1.4 million vascular grafts are needed every year in the US alone to replace diseased arteries. Of these, about 200,000 are small and medium diameter grafts (4-6 mm) for vascular access and to relieve lower limb ischemia and more than 600,000 are small diameter grafts (1-4 mm) needed for coronary bypass procedures. The conduit of choice for small diameter vascular graft surgery is the autologous vein or artery, but these are not available in 25-30% of patients due to preexisting conditions or previous harvesting [1]. Current grafts are made of polyethylene terephtalate (Dacron) or expanded polytetrafluoroethylene (ePTFE), or biologically derived conduits such as cryopreserved saphenous vein allografts and decellularized bovine ureters [2,3]. Synthetic grafts are being used successfully for replacements of large caliber arteries (above 8 mm internal diameter) with acceptable long term patency [4]. However, when the same materials are used in small diameter applications (less than 6 mm internal diameter), they perform very poorly as peripheral arteries, with 50% of them occluding within 5 years, potentially leading to amputation. This is due to the intrinsic thrombogenicity of the materials, significant compliance mismatch leading to peri-anastomotic intimal hyperplasia and lack of remodeling and growth when implanted in young patients [5]. Short term results of biological grafts are also quite promising, but despite their “off the shelf” appeal, poor 1-year patency, extended thrombosis, aneurysmal degeneration leading to rupture and calcification have limited the use of such conduits [6]. This daunting lack of options has prompted surgeons to implant small diameter vascular grafts made of synthetic polymers with suboptimal results.

Therefore, surgeons welcome the possibility of gaining access to “off-the-shelf” small diameter grafts that would be easy to suture, exhibit adequate compliance and burst pressures, remain patent and resist thrombosis and be resistant to aneurismal degeneration and calcification. It is believed that tissue engineering has the potential to generate such viable grafts by combining synthetic or naturally derived degradable or non-degradable scaffolds with a variety of cells followed by maturation in bioreactors. Such constructs have been tested in animal models but few of them have reached clinical trials because of their tendency to degenerate, dilate and calcify after implantation [6-9].

To overcome aneurismal degeneration and dilatation, we hypothesized that superior vascular graft scaffolds can be produced by chemically stabilizing acellular arteries. To test this hypothesis, we pioneered the use of elastin-rich tubular vascular grafts (ETVGs) produced from porcine arteries from which all cells and most of the collagen has been selectively removed. This approach has the advantage of creating a 3-D porous structure and maintaining native tissue architecture and arterial matrix "niche" while removing xeno-antigens. We were also the first to describe treatment with pentagalloylglucose (PGG) an elastin-stabilizing polyphenolic tannin to reduce biodegradation and calcification of ETVGs [10-12]. In addition we showed that PGG-treated ETVGs exhibited adequate mechanical and biological properties in vivo by subdermal implantation and were non-thrombogenic in acute implantation studies in rabbits [13,14]; recently we also showed that PGG treatment diminished the tendency of ETVGs to undergo diabetes-related alterations in vivo [10] which could become relevant if these grafts will be implanted in diabetic patients. Encouraged by these results, we are now for the first time presenting data regarding pre-clinical testing of stabilized ETVG grafts in a circulatory model in the rat using direct implantation as transposition grafts with 4 and 8 week follow up and indirect implantation using the isolation-loop approach with 12 week follow-up, a recently validated approach as a high throughput model for testing mechanisms of endothelialization [15].

Materials and methods

a) ETVG preparation, stabilization and characterization

Fresh porcine kidneys were obtained from the local abattoir and stored on ice while in transit back to the laboratory. The interstitial renal arteries (2.5-3.5 mm diameter, 10-15 mm length) were dissected, cleaned and decellularized by an alkaline treatment (0.1 M NaOH at 37 ºC for 3 h). Scaffolds were extensively rinsed with sterile ddH2O until the pH of rinse solutions dropped to about 8 and then finally rinsed in sterile PBS. Batches of scaffolds were further treated with sterile 0.1% pentagalloylglucose (PGG, Omnichem Ajinomoto, Belgium) in 50 mM phosphate buffer pH 5.5 containing 20% isopropanol for 24 h, rinsed and stored in sterile PBS. After sterilization for 24 h in 0.1% peracetic acid in sterile PBS, scaffolds were rinsed in sterile PBS and stored at 4º C for up to 3 months. Scaffold decellularization efficacy was qualitatively assessed by histology using DAPI nuclear staining and HematoxylineEosin (H&E) for cell nuclei and general matrix morphology, Masson's trichrome for collagen and smooth muscle proteins and Voerhoff van Gieson (VVG) stain for elastin and biotinylated GS lectin histochemistry for a-Gal [11]. DNA was also extracted from fresh arterial tissue and decellularized scaffolds using a Qiagen extraction kit and samples analyzed by PicoGreen assay and by ethidium bromide agarose gel electrophoresis.

b) Mechanical properties

For measurement of suture retention strength, ETVG samples were cut into 5 x 10 mm segments (n = 6 per group) and one end was clamped to a 10 N MTS test frame (MTS Systems Corp., Eden Prairie, MN). A single 4-0 braided suture was placed 1 mm from the free edge and its end tied to the MTS test frame. Samples were then preloaded to 0.005 N and extended to failure at 5 mm/min; final data was expressed as grams-force.

For compliance and burst pressure analysis, ETVGs (n = 6 per group) were adapted on both ends with barbed Luer connectors and secured with a clamp at each connector. A peristaltic pump was used to

progressively fill sections with PBS at room temperature and a pressure transducer was mounted on the distal end of the arterial scaffold to record pressures continuously via a computer interface. For diametrical compliance, segments were exposed to 80 mmHg and 120 mmHg and digital images were captured at each pressure setting. The images were then imported into SolidWorks and mean outside diameter calculated digitally using measurements at 6 positions perpendicular to the ETVG sides. Diametrical compliance was then calculated using equations published by Hamilton's group [16]. A similar setup was used to assess burst pressures (*n*=6 per group) using the peristaltic pump to progressively fill sections with PBS until rupture.

c) Scaffold heparinization

To optimize the heparinization protocol, PGG and non-PGG treated ETVG samples were rinsed in phosphate buffered saline (PBS), reacted with Jeffamine, amineterminated polypropylene glycol, (Huntsman) 240 mM in 0.25 M MES buffer, pH = 5,2 h at room temperature using a combination of 1-Ethyl-3-(3 dimethylaminopropyl) carbodiimide and N-hydroxysuccimimide (EDC/NHS, 300/ 10 mM) as activator. After another PBS rinse, nitrous acid degraded heparin (Celsius; 2 mg/ml; in 0.15 M NaCl; pH=3.9, solution containing 1 mg/ml $NaCNBH_3$) was coupled by reductive amination to the aminated and non-aminated control samples by a 16 h reaction at room temperature. The treatments were performed either with or without pre-soaking in Heparin and samples were subsequently rinsed and stored in sterile PBS.

d) Heparin quantification

The heparin content of ETVGs (*n* = 3) was quantitatively determined by 3methyl-2-benzothiazoninone hydrazone (MBTH) assay adapted from Risenfeld and Roden [17] similar to that described before by Bezuidenhout et al. [18]. Heparin content (mg/g tissue) was calculated from standard curves.

e) Heparinization of grafts for implantation

Heparinized ETVG samples for implantation were prepared as described above via Jeffamine functionalization (without pre-soaking) and heparin attachment using 0.2µm-filtered solutions under sterile conditions in a laminar flow hood. The following four implant groups were thus generated: 1) untreated

(None); 2) PGGtreated (PGG); 3) Heparin (Hep); and 4) PGG followed by Heparin (PGG, Hep).

f) Denaturation temperature determination

Thermograms of ETVG samples (5-10 mg, *n* = 3) in sealed aluminum sample pans were obtained at a heating rate of 10 ^{o}C/min (DSC 7; Perkin Elmer) and the onset temperature of the denaturation endotherm recorded as the denaturation temperature [19].

g) Resistance to enzymatic degradation

ETVG samples (*n* = 6 per group and per enzyme) of about 3 x 3 mm were lyophilized and their masses recorded to obtain dry tissue mass. For collagenase resistance, samples were incubated in 1 ml solution of 20 units/mL ultrapure type VII collagenase (Sigma) in 1 mM $CaCl_2$ 100 mM Tris (hydroxymethyl) aminomethane at pH 7.8 and 0.02% NaN_3. For elastase resistance, samples were incubated in 1 ml of 6.25 units/mL ultrapure elastase (Elastin Products Company) in the same buffer.

After incubation at 37 ^{o} C for 24 h with mild agitation, samples were centrifuged at 12,000 RPM, rinsed three times with ddH_2O, lyophilized and weighed to calculate percent mass loss during enzyme digestion.

h) Implant groups

For direct implants, a total of 52 rats were implanted with vascular grafts to complete a targeted *n*=12 per ETVG group, with *n*=6 per time point. Three rats were replaced due to premature graft rupture at 6 weeks. For isolation-loop implantation, we first prepared two groups of 2.5-3 mm diameter, 10-15 mm long acellular grafts, namely Hep and PGG, Hep (*n*=6 per group) as described above. Then we heat set 90 mm long low-porosity ePTFE segments for 3 min at 100^{o} C over a spiraled 1.5 mm nylon cord to generate a stable alpha-loop structure without kinking. A 10 mm midway segment was then removed from the ePTFE loop and replaced with a ETVG segment by end-to-end anastomosis with interrupted 90 nylon (Ethilon; Johnson & Johnson, New Brunswick, NJ) using an operating microscope (Zeiss Universal S3 OPMI 6-SFC,

Oberkochen, Germany).

i) Graft implantation

All animal experiments were approved by the Animal Research and Ethics Committee of the University of Cape Town and were in compliance with the Guide for the Care and Use of Laboratory Animals, Institute of Laboratory Animal Resources, Commission on Life Sciences, National Research Council, South Africa. Male Wistar rats weighing 350-510 g were induced with isoflurane 5% anesthesia and were maintained with 2% isoflurane spontaneously breathing via a conical mask. Sterility was maintained throughout the procedure and a warming pad was used to regulate temperature. Following a mid-line laparotomy, the aorta was dissected free of the inferior vena cava and surrounding tissues and all perforating arteries between the left renal artery and the iliac bifurcation were ligated. In all cases the inferior mesenteric artery was preserved. A single dose of intravenous heparin (1 mg/kg) was administered and the direct grafts were implanted into the infrarenal aorta by end-to-end anastomoses using 9-0 Nylon interrupted sutures. The isolation-looped grafts were similarly implanted by anastomoses to the infrarenal aorta and further secured with a suture to the lumbar muscles to prevent twisting. The abdomen was closed in layers and Buprenorphine (0.1 mg/kg) was administered subcutaneously twice daily for three days. No anticoagulation medication was administered after surgery.

j) Graft removal

Following 4 and 8 weeks for direct implants and 12 weeks for isolation-loop implants, the abdomen was opened and the grafts inspected for patency by observation of pulsation in the distal aorta, under general anesthesia as for the implant procedure. Animals were euthanized by exsanguination following 1 mg/kg heparin administration via the inferior vena cava. The aorta was flushed with phosphatebuffered solution via the apex of the left ventricle until clear of blood (cca.150 ml), following which the aorta was perfusion fixed with formalin. The graft was then excised, cross-sectioned for macro-photography and processed for histology.

k) Histology and quantification

Tissue samples were post fixed in zinc solution [20], dehydrated, embedded in paraffin, sectioned and processed for histological examination. HematoxylineEosin and Miller and Masson's trichrome stain (ELMAS) were used for basic light histological analysis. Immunofluorescent identification of endothelial cells was performed with antibodies to Factor 8 (Dako), CD3 for lymphocytes (Dako), ED1 for pan-macrophages (Serotec), CCR7 for M1 macrophages (Abcam), ED2 for M2 macrophages (Serotec), alpha-smooth muscle cell actin (Dako), using Cy3 conjugated streptavidin or Alexa Fluor 488 GxR (Invitrogen). Immunohistochemistry for endothelium was also performed with anti-CD31 antibodies (Fitzgerald). Elastin and calcification was identified with Orcein and Alizarin red stain respectively, and glycosaminoglycans were stained with Alcian blue. Quantitative measurements of wall thickness, lumen area, internal elastic lamina (IEL) diameter and neo-intimal pannus overgrowth were performed on trichrome stained sections with Visiopharm Integrated Systems software (VIS, Visiopharm A/S, Hoersholm, Denmark) and Adobe Photoshop CS6 on mid-graft cross-sections.

l) Statistical analysis

Statistical tests were performed with STATA (StataCorp. 2011. *Stata Statistical Software: Release 11* College Station, TX: StataCorp LP) Results were expressed as mean ± SD for continuous variables. All continuous data was confirmed as nonparametric (Shipiro-Wilkinson) interrogated with Mann Whitney test for statistical significance. Kruskal-Wallis equality-of-populations rank test was used for multiple group analysis. Categorical data was tested with the Fishers exact, and the level of significance was set at $p < 0.05$. Burst pressures, diametrical compliance and enzyme resistance were compared using ANOVA, and effect of heparinization and denaturation temperatures with student's *t*-test.

Results

a) Scaffold preparation and characterization

To generate 2.5-3.5 mm diameter, 10-15 mm long vascular grafts, we dissected segmental and inter-lobar arteries from adult porcine kidneys and decellularized them with NaOH as reported previously with minor modifications [21]. Completeness of decellularization was confirmed lack of extractable DNA, absence of cell nuclei in histological DAPI staining (Fig. 1) and histological analysis including H&E, Trichrome, and a-Gal antigen lectin histochemistry, all of which depicted cells in native tissues and their absence in decellularized ETVGs. Acellular renal arteries showed good pres-ervation of overall arterial matrix morphology including native collagen and elastin (Fig. 1). Notable histological features of the acellular renal arteries included a distinct internal elastic lamina (IEL), a relatively thin media containing thin elastin and collagen fibers and a very thick elastin and collagen-rich adventitia. Suture retention strengths and burst pressures of acellular arteries were not different from those of native arteries (Fig. 2). However, decellularization reduced diametrical compliance by about 50% (Fig. 2).

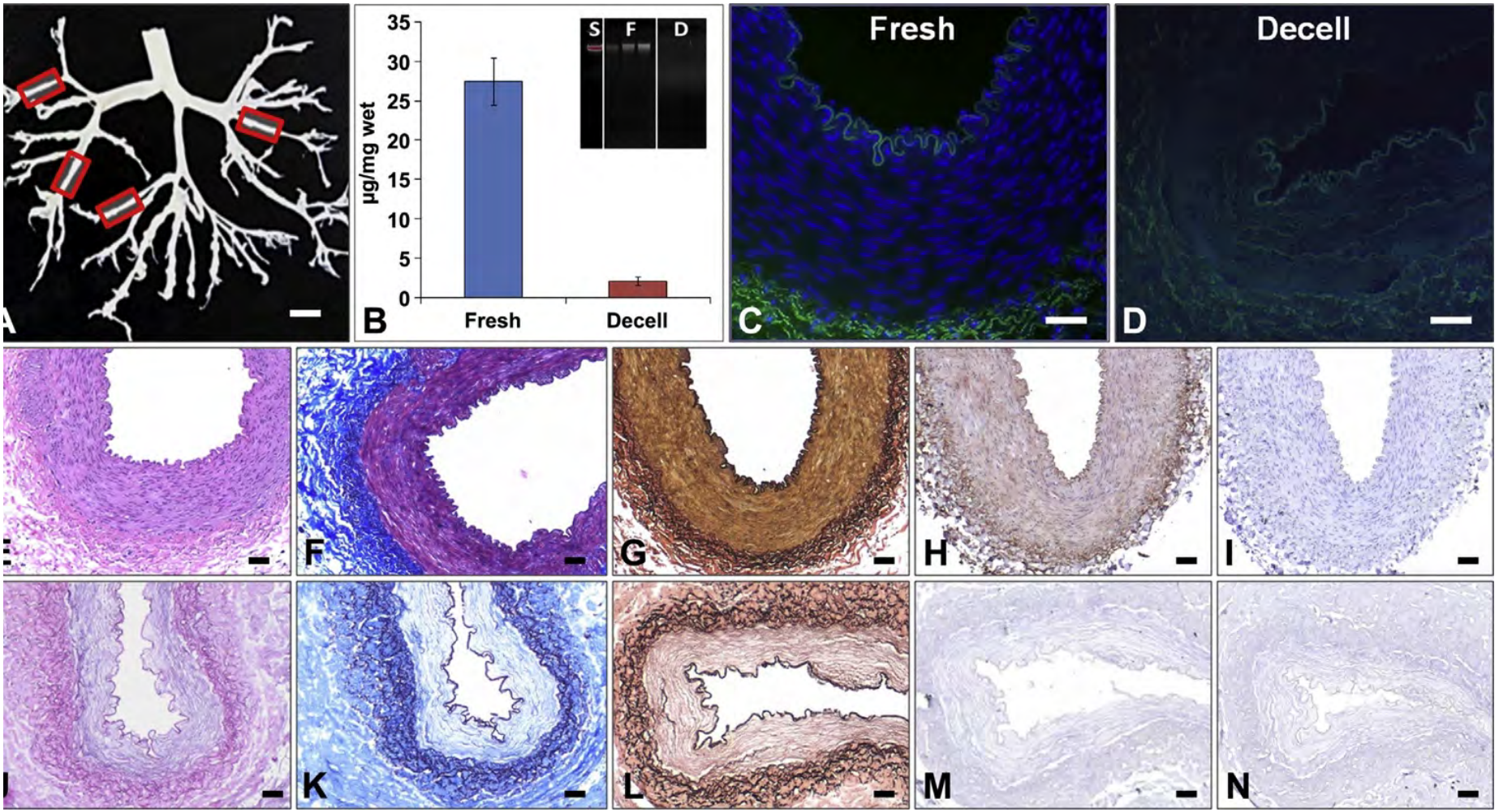

ure 1 Vascular scaffold data. (A) A whole porcine kidney arterial tree is shown after it was dissected and cleaned manually. Segmental and interlobar arteries (red squares) of 3 mm diameter and 10e15 mm length were dissected and decellularized as described in the manuscript. Bar is 10 mm. (B) DNA was extracted from fresh and decellularized ecell) arteries and quantified using Picogreen (mg/mg, n=6 samples per group) and verified with ethidium bromide agarose gel electrophoresis (insert, n=3, S, DNA standard; F, sh; D, decellularized). (C) DAPI nuclear stain (blue) superimposed over green elastin autofluorescence was used to highlight cells in fresh arteries and (D) lack of cells in cellularized (Decell) grafts. Images are representative for n=6, bars are 50 mm. Lower panels show histology of fresh (EeH) and decellularized (JeM) arteries using H&E, (E, J), sson's trichrome (F, K), Verhoeff van Gieson (G, L), and a-Gal histochemical detection using GS lectin (H, M). Images are representative for n=6 per group, bars are 50 mm. N) are a-Gal histochemistry negative controls for fresh and Decell, respectively. (For interpretation of the references to color in this figure legend, the reader is referred to the b version of this article.)

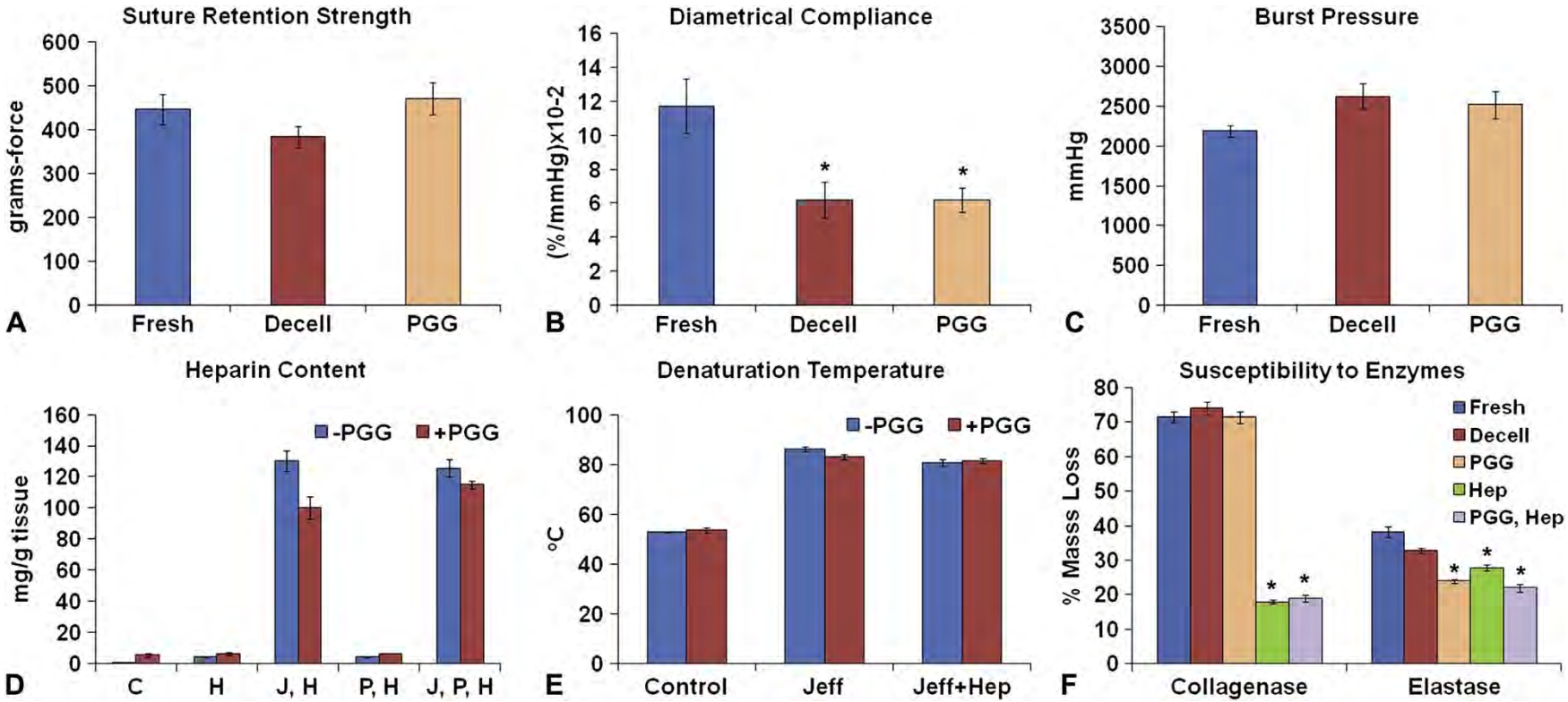

*Figure 2 Characterization and stabilization of acellular arterial scaffolds. (A) Suture retention strength, (B) diametrical compliance and (C) burst pressure values for fresh arteries, decellularized (Decell) arteries and PGG-treated Decell arteries (PGG). Data was obtained from n=6. *-statistically significant as compared to fresh, $p < 0.05$. (D) Heparin content of untreated ETVGs (-PGG) and PGG treated scaffolds (þPGG). Groups were: Controls (C) not subjected to treatments, (H) treated with activated heparin alone and treated with Jeffamine (J) with and without pre-soaking in heparin (P). (E) Graft crosslinking as evaluated by DSC test for untreated (-PGG) and PGG treated samples (þPGG) before (Control) and after treatment with Jeffamine (Jeff) or Heparin (Hep), or Jeff followed by Hep (Jeff þ Hep). (F) Five ETVG groups were prepared and tested for resistance to enzymes: fresh renal arteries, decellularized arteries (Decell), and Decell treated with PGG alone (PGG), Heparin alone (Hep), and PGG followed by Hep (PGG, Hep). n=6 per group; *-statistically significant as compared to Decell, $p < 0.05$.*

Table 1 Summary of direct grafts

	4 w	8 w	Ruptured	Replaced	Survival at 4 w (%)	Survival at 8 w (%)	Excluded[a]	Analyzed
Non	6	8	2	2	85	92	2[b]	12
PGG	6	8	1	1	100	100	3[c] + 1[b]	10
Hep	6	6	0	0	100	100	1[c]	11
PGG, Hep	6	6	0	0	100	100	0	12

a Excluded from quantitative analysis:
b Ruptured grafts (n=3).
c Grafts explanted at designated time points which exhibited outside diameter >3.5 mm and an aortic to graft diameter ratio <0.4 at implant.

b) Stabilization and heparinization

To increase biocompatibility, untreated and PGG-treated ETVGs were heparinized by covalent immobilization of nitrous acid activated heparin (which contains aldehyde end-groups for end-point attachment). To monitor efficacy, we measured heparin content in each group of tissues. Simple soaking in activated heparin did not result in heparin binding because acellular arteries did not contain sufficient exposed amine groups. Thus, we first aminated the ETVGs using diamines (Jeffamine) and carbodiimide chemistry. Control samples showed low baseline levels of heparin, irrespective of PGG treatment. No differences were seen between the tissue samples which were pre-soaked in heparin or not (Fig. 2). Significantly and much higher heparin content values were observed for samples that were first aminated with Jeffamine/carbodiimide prior to the reaction with heparin. PGG did not interfere with the reaction, and pre-soaking in heparin did not significantly affect the heparin content of ETVGs (Fig. 2). Jeffamine/carbodiimide treatment alone resulted in significant increases in denaturation temperature ($p < 0.001$) of the grafts (Fig. 2) indicative of crosslinking. Further reaction of aminated scaffolds with activated heparin did induce further chemical crosslinking in both -PGG or þPGG scaffolds. These results indicate that covalent immobilization of heparin cross-links the ETVGs and that PGG does not impede heparinization. Analysis of resistance to collagenase and elastase showed that decellularization did not significantly change tissue susceptibility to enzymes ($p > 0.05$). PGG treatment of ETVGs reduced their susceptibility to elastase by about 50% while heparinization stabilized collagen by more than 80% (Fig. 2), indicating that PGG stabilizes elastin while heparinization treatment cross-links collagen.

c) Direct implants; surgical handling and implants statistics

Although the surgeon was not blinded at the time of graft implant, surgical handling was adequate for all vascular grafts and subjectively superior in the heparinized set of grafts (Hep and PGG, Hep groups). The goal of this study was to ensure completion of $n = 6$ implants per time point per group. The implant statistics

(Table 1) show that only 3 grafts ruptured prior to their scheduled 8 week explant, all of which occurred after 6 weeks. Two of them were from the non-stabilized graft group ("Non") and one from the PGG-treated group. Rupture was confirmed at autopsy with abdominal blood and macroscopic evidence of wall defect. These grafts were subsequently replaced. After replacement, all of the animals survived to their designated explant time points and had 100% patent grafts (Table 1). An overview of implantation and explanation macroscopic aspects is shown in Fig. 3.

Direct implants; histological evaluation

All grafts, irrespective of the treatments they were subjected to, demonstrated concentric peri-graft tissue infiltration and formation of a well vascularized collagenous granulation tissue of about600e800 mm in thickness (Fig. 4). Cells were seen infiltrating and completely re-populating the (initially acellular) graft adventitiawithout penetrating the media. This cellular infiltration was composed of CCR7-positive (M1) and ED2-positive (M2) macrophages, a-smooth muscle cell actin-positive myofibroblasts, foreign body giant cells and very few CD3-positive lymphocytes (Fig. 4). The thickness of this capsule did not increase from 4 to 8 weeks and did not appear to reduce the lumen diameter, suggesting little if any constrictive remodeling. A thin layer of neo-intimal tissue with the appearance of "intimal hyperplasia" but probably derived from peri-anastomotic pannus overgrowth, was also present in all direct implants. The neo-intimal tissue was rich in myofibroblasts and covered by a continuous layer of F8-positive endothelial cells (Fig. 4). In most explants

analyzed, the neo-intimal tissue was stable and prevented formation of clots. However, in about 1/3 of all implants, irrespective of graft pre-treatment, the neo-intimal tissue underwent detachment or remodeling at 4 weeks, allowing for thrombus formation. At 8 weeks, the heparizined grafts (with or without PGG) did not exhibit any thrombus formation. Three neointima samples (out of total 45 analyzed) also exhibited chondroid metaplasia with Alcian Blue positive (not shown) and Alizarin Red positive structures (Fig. 4). Two additional samples stained positive for calcium in the neointima, in the absence of chondroid metaplasia. None of the acellular grafts showed any evidence of calcium deposition within the implanted graft wall.

To gather more quantitative data, we analyzed representative ELMAS-stained midway graft sections by digital morphometry and measured the perimeter of the IEL, wall area, lumen area, wall thickness and neo-intimal pannus area for each sample (Fig. 5). We also used Orcein stain for elastin and quantified the integrity of implanted elastin as a function of graft treatment. When compared to pre-implant samples, the IEL diameter in all implanted grafts (irrespective of treatment) did not change after 4 weeks but increased significantly to almost 100% at 8 weeks in non-treated grafts (Fig. 6). The IEL diameters in grafts treated with PGG, Hep or PGG followed by Hep remained unchanged at 8 weeks ($p > 0.05$). Similarly, the luminal area was statistically larger only in the non-treated grafts at 8 weeks; grafts treated with PGG alone, Hep alone or PGG followed by Hep exhibited similar luminal areas

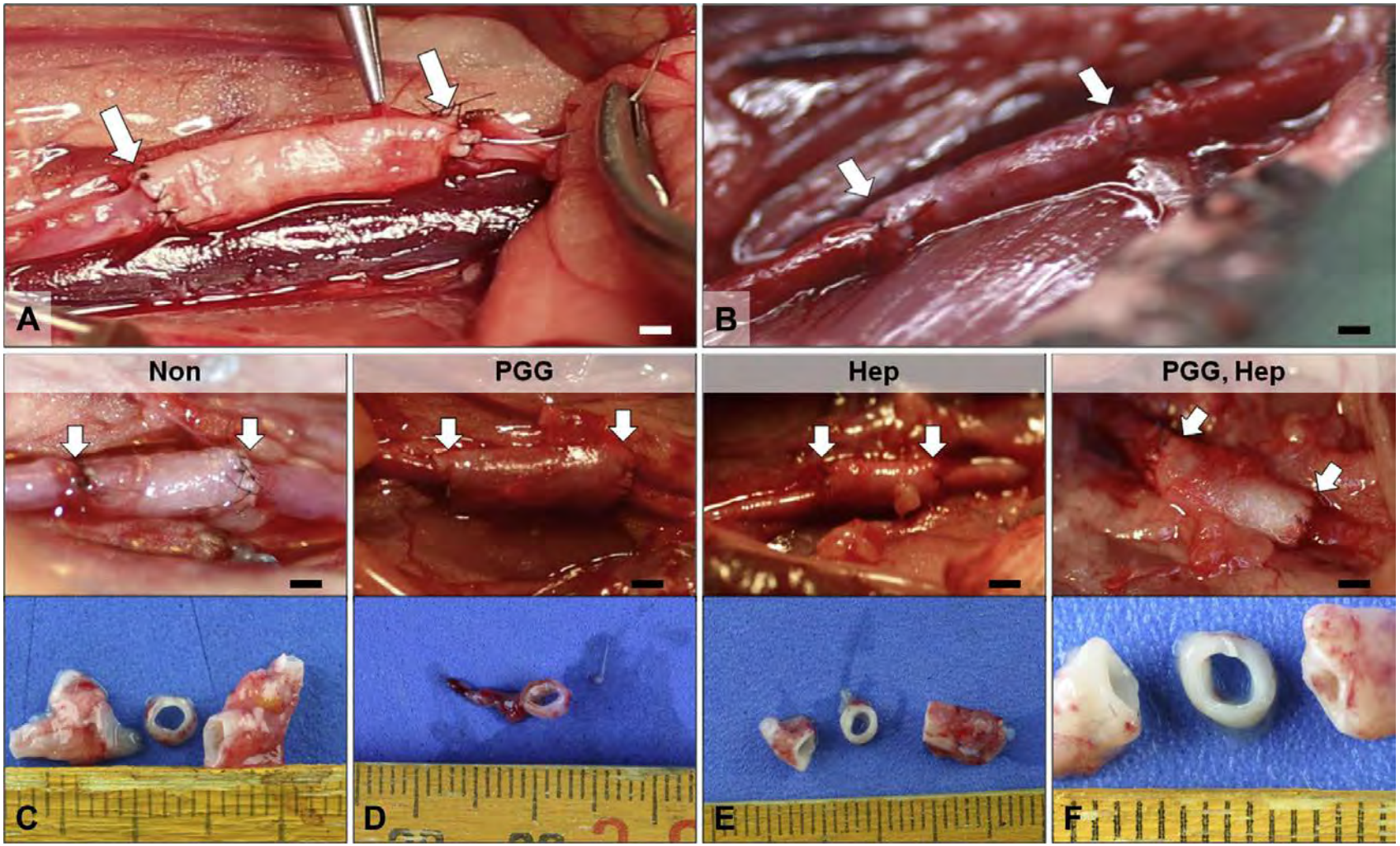

Figure 3 Intra-circulatory implantation of ETVGs as direct grafts. (A-B) macroscopic images showing grafts during implantation in the rat infrarenal abdominal aorta; white arrows depict the anastomoses; bar is 1 mm. (C-F) representative macroscopic aspects of grafts before explantation (top) and macro images of midsections after perfusion fixation of corresponding grafts in each group (bottom). The groups were ETVGs without pre-treatment (Non) or treated with PGG alone (PGG), Heparin alone (Hep), and PGG followed by Hep (PGG, Hep). White arrows depict the anastomoses and bar in (C-F) is 1 mm.

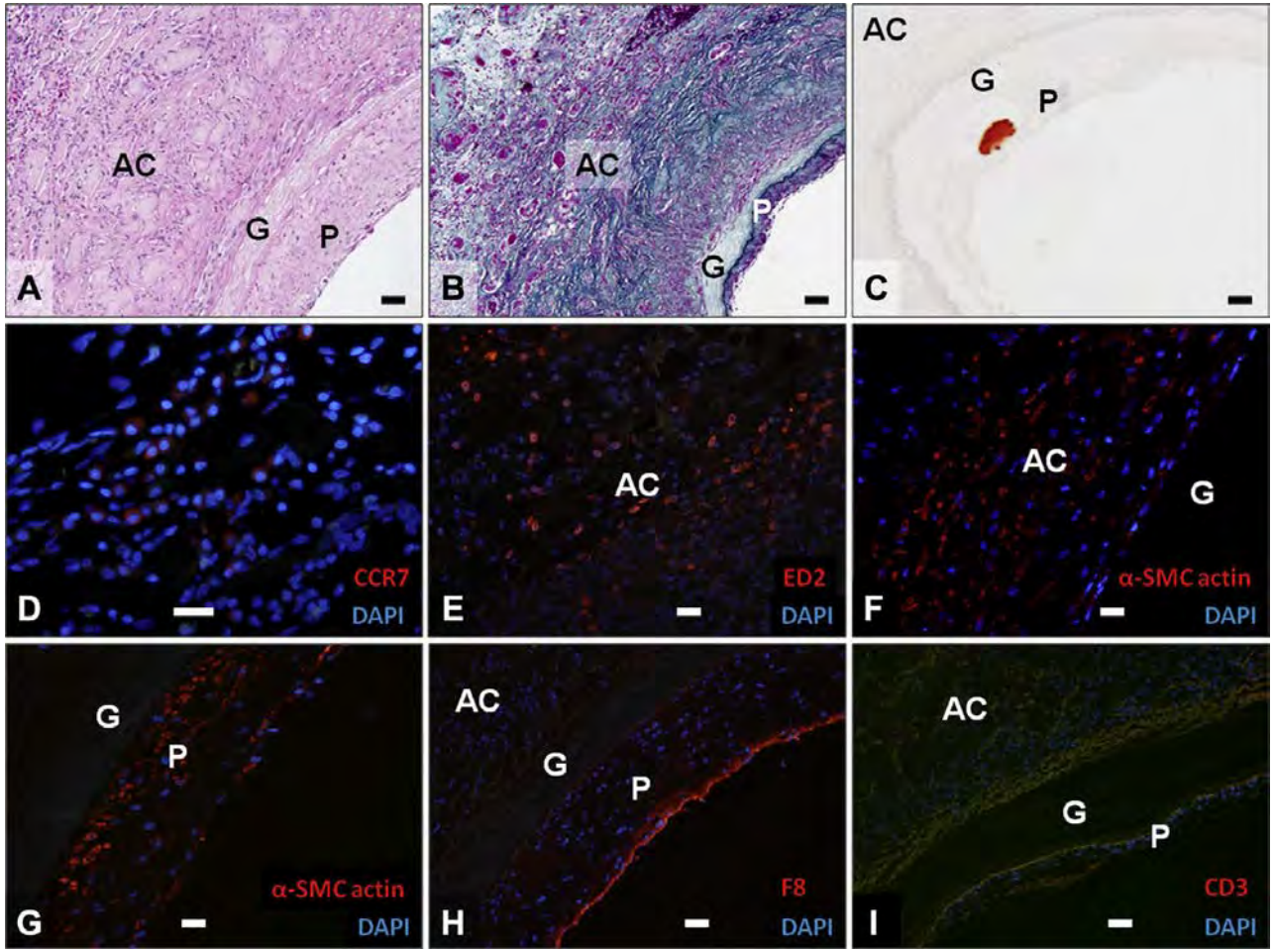

Figure 4 Histology of explanted direct grafts. Representative sections shown after staining with (A) H&E, (B) Masson's trichrome, (C) Alizarin red, (D) CCR7 immunofluorescence (red) for M1 macrophages, (E) ED2 stain (red) for M2 macrophages, (F) a-smooth muscle cell actin (red) for activated myofibroblasts in the adventitia and (G) in the neo-intima; (H) F8 endothelial stain and (I) CD3 lymphocyte stain. (DeI) nuclei were counterstained with DAPI (blue); Images are representative for n=6, bars are 50 mm. AC, adventitial capsule; G, initial graft; P, neo-intimal pannus. Lumen is at lower right in all images. (For interpretation of the references to color in this figure legend, the reader is referred to the web

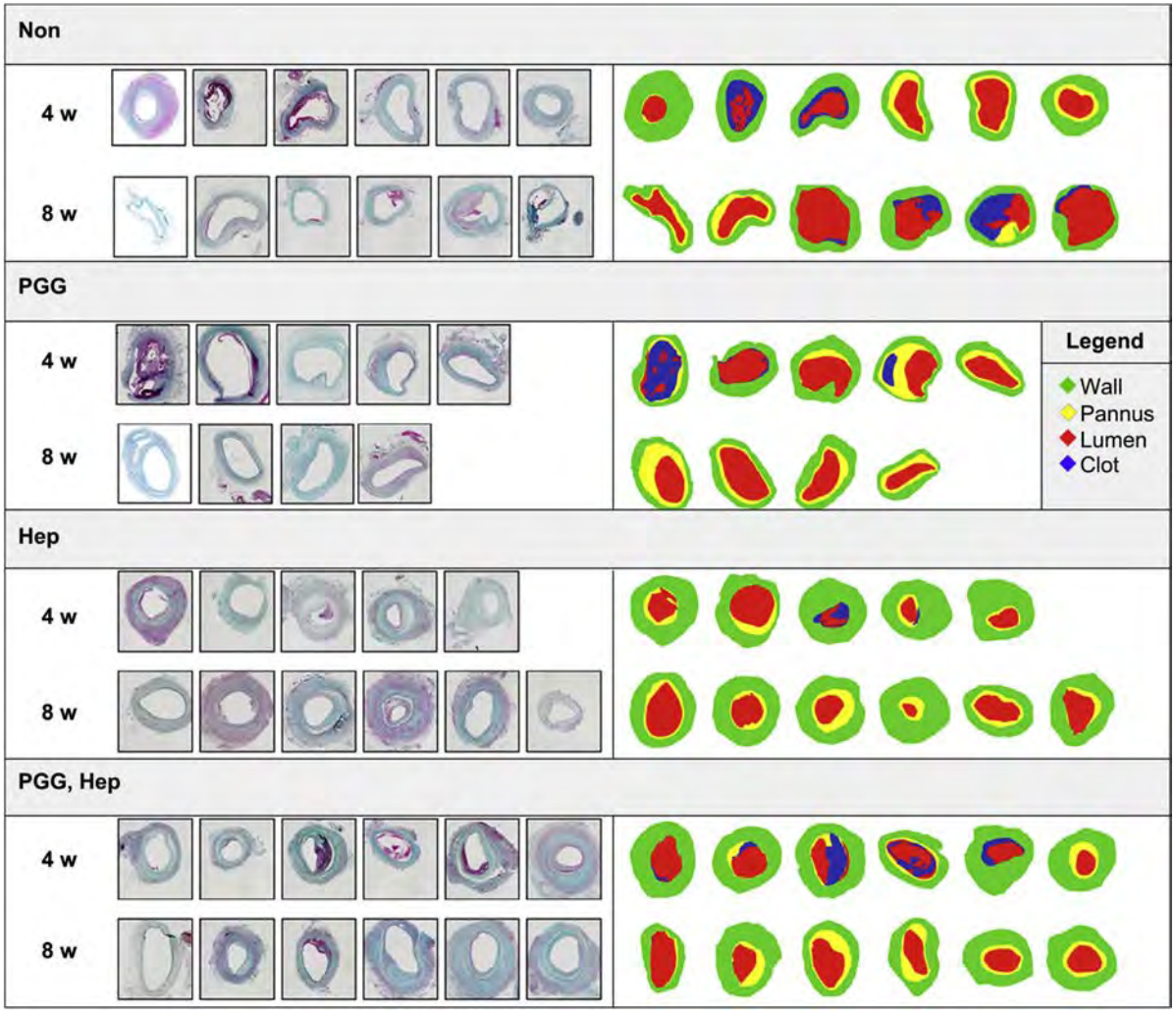

Figure 5 Evaluation of explanted direct graft histology. Panel of representative Masson's stained mid-graft histology cross-sections from each individual implant retrieved at 4 weeks (4 w) and 8 weeks (8 w). ETVG groups were: untreated (Non), PGG-treated (PGG), Heparin treated (Hep) and PGG followed by Heparin (PGG, Hep). Histology images were digitized and color coded to measure wall thickness (green), pannus area (yellow), lumen area (red) and clot (blue). Stained sections are shown at left and corresponding digitized images at right. (For interpretation of the references to color in this figure legend, the reader is referred to the web version of this article.)

at 4 weeks without signs of progression at 8 weeks ($p > 0.05$). The graft wall thickness (collagenous granulation tissue) was similar in most groups (600-800 mm) except for PGG, where it was thinner ($p < 0.01$). Neo-intimal pannus thickness increased across all four groups from 4 weeks to 8 weeks as a result of peri-anastomotic tissue ingrowth (Fig. 6); however the differences among the four groups at 8 weeks were not statistically significant. Notably, statistically significant preservation of elastin with sequential stabilization treatments was measured in ETVGs (Fig. 6E). Both heparinization and PGG treatment independently resulted in a statistically significant improvement in elastin preservation (when compared to untreated controls) with an additive effect in their combination demonstrating that elastin, unless stabilized, is susceptible to in vivo degeneration. Elastin stabilization only correlated statistically to dilatation at 8 weeks (Bivariate Fit, p=0.0427).

Evaluation of isolation-loop (indirect) implants

To test the hypothesis that the neo-intimal pannus observed in direct implants is related to trans-anastomotic tissue ingrowth an not to transmural cell infiltration, we sutured 10 mm-long graft segments midway in 9 cm long ePTFE loops such that the implanted grafts were 4 cm away from the anastomosis to the native abdominal artery (Table 2). The grafts were easy to suture onto the ePTFE material and they did not kink when forced into an alphaloop configuration (Fig. 7). At explantation, the grafts were well integrated into host tissues, namely the retroperitoneum. In the Hep group 5/6 grafts were patent while in the PGG, Hep group 4/6 grafts were patent.

Similar to the direct implants, all isolation-loop grafts demonstrated formation of the external, well vascularized collagenous granulation tissue (Fig. 7). Quantitative morphometric comparisons between the two pre-treatments applied to the indirect grafts (Hep vs PGG, Hep) showed that there were no significant differences in wall (capsule) thickness, IEL diameter (dilatation), elastin preservation and lumen area ($p > 0.05$). Similarly, no statistical differences were noted in these four parameters when indirect implant data were compared to the direct implant results. The major differences between direct and indirect grafts were 1) the complete lack of neo-intimal pannus tissue formation in the isolation-loop

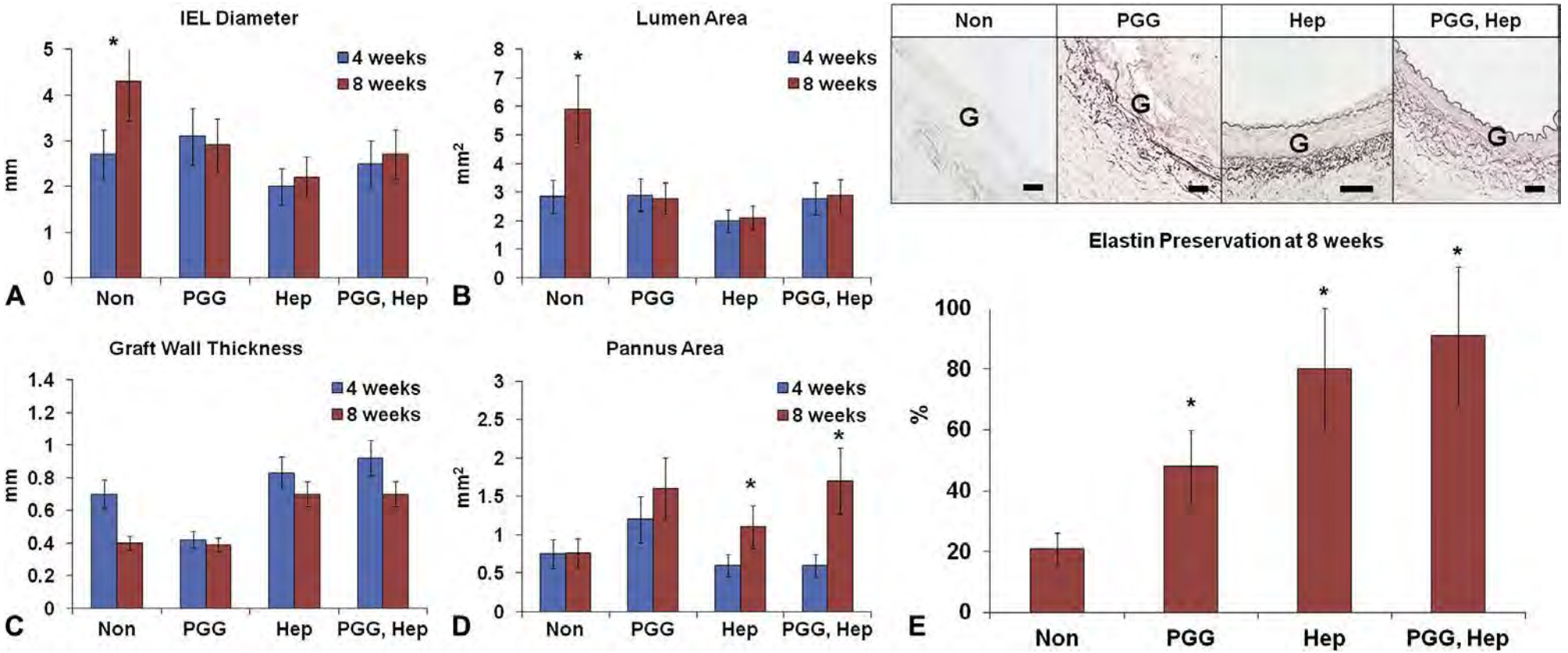

*Figure 6 . Quantitative morphometric data obtained from direct implants. Digitized images (as shown in Fig. 5) were used to measure: (A) IEL diameter, (B) lumen area, (C) graft wall thickness and (D) pannus area in untreated ETVGs (Non), PGG-treated (PGG), Heparin treated (Hep) and PGG followed by Heparin (PGG, Hep). *-statistically significant as compared to 4 weeks, $p < 0.05$. (E) Orcein stain for elastin (top row) and quantification of elastin content from the histological images (bottom). *-statistically significant as compared to non-treated scaffolds (Non), $p < 0.05$. G, graft. Lumen is at top or top/right corner, bar is 50 mm.*

Table 2 Summary for isolation-loop (indirect) grafts.

	Implanted	Ruptured	Patent	Analyzed
Hep	6	0	5	5
PGG, Hep	6	0	4	4

samples, irrespective of the graft pre-treatment and 2) significantly reduced thrombus formation. Since the arterial sub-endothelial basement membrane in the indirect grafts was not covered by pannus, this experiment also gave us the unique opportunity to evaluate the intrinsic thrombogenicity of the luminal surface of acellular arteries. As seen in the histology, immunofluorescence and SEM images, the surface of the 12 week indirect implants appeared wavy but relatively smooth and free of adhered cells, fibrin strands or microthrombi (Fig. 7).

Discussions

We have shown earlier that alkaline decellularization of carotid segments removes all cells and some of the collagen; however, the NaOH technique was never applied to muscular arteries. Current results on renal arteries demonstrate that the alkaline decellularization method was effective, with complete cell removal as seen on DAPI stained sections and lack of extractable DNA, as well as lack of cells on histology stains (H&E, trichrome, VVG). Furthermore, acellular arteries lacked a-Gal staining which confirmed complete decellularization and also revealed the absence of the powerful xeno-antigen throughout the tissues.

We chose renal arteries as the tissue source in order to generate size-matched grafts which would be implanted into the abdominal artery of rats. In current studies we focused on acellular arteries as biological scaffolds for several reasons. First, because we believed that the biggest asset of acellular scaffolds prepared from target tissues is the presence of an architecturally accurate extracellular matrix network capable of presenting cell adhesion motifs for repopulation with differentiated cells as well as to serve as "niches" and cues for stem cell differentiation into desired cell types [22,23]. While cell removal reduced immunogenicity and generated pores allowing cell infiltration, it also raised concerns regarding the exposure of the vascular sub-endothelial layer to flowing blood. In current studies we showed that the sub-

endothelial basement membrane of ETVGs was essentially non-thrombogenic. Second, preservation of major tissue components (elastin and collagen) in their original configuration ensured adequate mechanical properties. Our results showed that suture retention strength, handling properties and burst pressures were unaltered by decellularization, while compliance values were reduced by about 50% as compared to fresh arteries. These results suggest that load-bearing structural components were well preserved, while other elements responsible for recoil (elastin associated microfibrils, proteoglycans) were probably removed by decellularization. We and others have shown that among matrix components, the proteoglycans are rapidly lost during decellularization [14]. It remains to be determined whether these compliance levels (5-6%) will be important in the long run; however these values are similar to those reported by Hamilton's group for human femoral and popliteal arteries (4.70-6.1%) [16]. Third, maintenance of intact, mechanically functional elastin within the structure of scaffolds is a very important aspect of vascular tissue engineering. Elastin is almost impossible to incorporate into sheets or lamellae using a bottomeup approach and new mature elastin fibers are notoriously difficult to synthesize in vitro or in vivo [24,25]. Elastin is important for recoil properties of arterial tissues and thus its presence within our scaffolds may ensure extended mechanical durability. Moreover, elastin has a tendency to calcify and degenerate upon implantation and once lost in vivo, it will not likely be re-synthesized by resident or infiltrating cells. For this reason we used arteries as a starting material. After decellularization, elastin is evident in the form of a distinct layer in the IEL, as fine fibrils within the media and as an extensive 3D network of fibers within the adventitia. We then chose to treat ETVGs with PGG, an elastin binding polyphenol which reduces elastin's susceptibility to enzymatic degradation and also diminishes its calcification potential [11,21,26-29]. Recently we also showed that PGG treatment of elastin-rich scaffolds protected implants from diabetes-related glycation, crosslinking and alterations in mechanical properties, which might prove very beneficial for diabetic patients requiring peripheral vascular surgery [10].

Acellular arterial scaffolds derived from renal arteries also contained a significant amount of collagen specifically in the adventitia layer. In order to stabilize the collagen component and to increase implant hemocompatibility, we heparizined the scaffolds via carbodiimide chemistry. The optimal protocol employed Jeffamine/carbodiimide tissue amination, followed by reaction with activated heparin, which yielded incorporation of significant amounts of heparin within the ETVGs (about 10% heparin by tissue weight). Results also showed that PGG did not interfere with the heparinization reaction and that collagen

was effectively crosslinked as evidenced by increased denaturation temperatures. Resistance to enzymatic degradation further confirmed that PGG stabilized elastin by reducing its susceptibility by almost 50%. This effect was demonstrated earlier by us for grafts derived from carotid arteries [21]. Heparinization stabilized and crosslinked collagen and increased its resistance to collagenase by 3e4 fold. Using these two selective stabilization techniques, we generated 4 main scaffold groups which were selected for implantation as direct transposition grafts in the abdominal aorta of rats and analyzed after 4 and 8 weeks: untreated, PGG-treated (elastin stabilized), hepariized (collagen stabilized) and PGG, heparin treated (elastin and collagen stabilized). Initial studies showed that the scaffolds exhibited good handling properties and were easy to implant. Survival was above 85% reaching 100% in some groups and overall patency at explantation was close to 100% in all groups. Samples were analyzed by histology and the findings of this study could be separated into two categories; those which were unrelated to the implant treatment and those specific to the implant.

In the first category, one major finding was encapsulation of the grafts in a concentric, peri-graft vascularized granulation tissue which integrated well with the scaffold adventitia but not the media. The newly formed collagenous tissue stabilized at about 800 mm thickness after a few weeks and did not grow in thickness with time. It is known from previous work by Campbell et al. that implantation of solid objects (rods, tubes) into the peritoneal cavity or pleural cavity induces activation of macrophages and initiation of a foreign body response [30,31]. Infiltrating cells differentiate into myofibroblasts which generate a new connective tissue capsule rich in collagen surrounding the implant. These collagen tubes were later used as vascular grafts with promising results [30,31]. A similar approach was used to manufacture heart valves by implanting tricuspid valve-shaped molds subdermally in rabbits and detaching the collagenous capsule tissue [32]. In pilot studies, we also observed that essentially the same type of capsule is formed when ETVGs are implanted as direct vascular grafts in the femoral artery in minipigs (data not shown); thus it appears that this encapsulation reaction is non-specific and could beneficial after implantation of tubular grafts. Notably, porcine ETVGs did not elicit an immune reaction after implantation in rats, strengthening

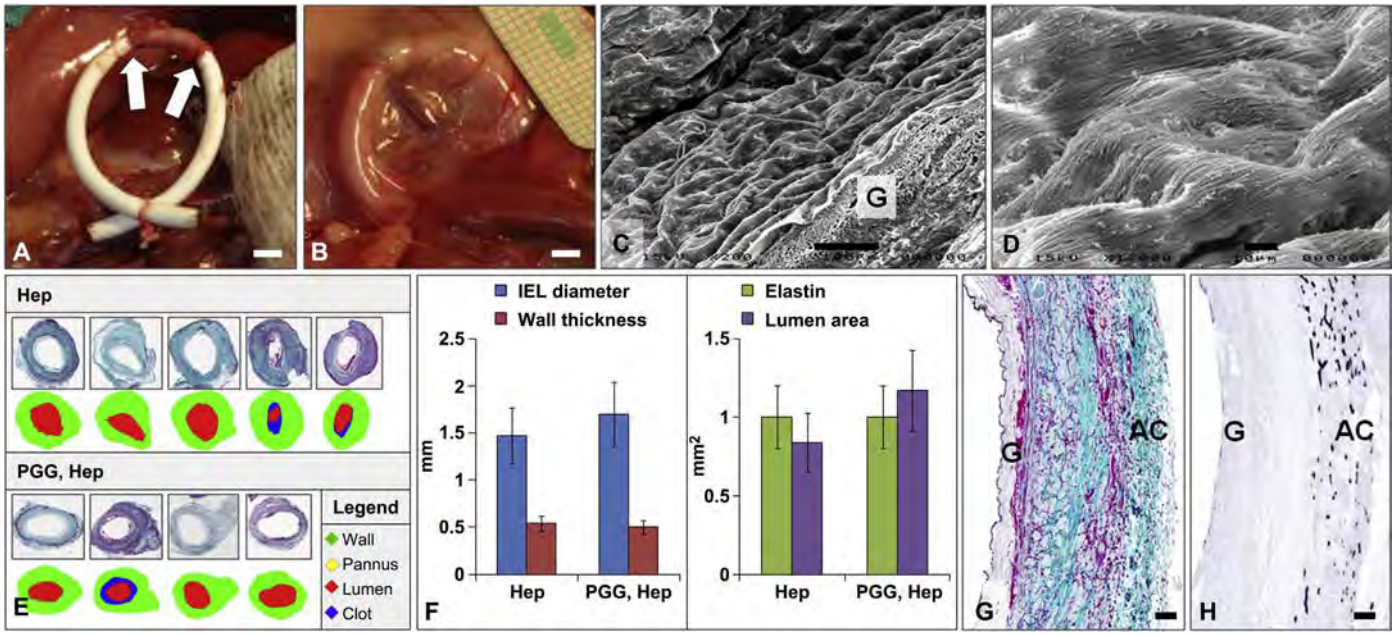

Figure 7 Indirect isolation-loop graft evaluation. (A) Macroscopic image of indirect graft during implantation in between two ePTFE looped segments (white) and (B) at explantation. Bar is 3 mm. (C, D) SEM analysis of the scaffold lumen surface after 12 weeks implantation. G, cross section of the graft. Bar is 100 mm in (C) and 10 mm in (D). (E) Panel of representative Masson's stained mid-graft histology cross-sections from each individual implant and ETVG group: Heparin treated (Hep) and PGG followed by Heparin (PGG, Hep). Histology images were digitized and color coded to measure wall thickness (green), pannus area (yellow), lumen area (red) and clot (blue). Stained sections are shown on top and corresponding digitized images below them. (F) Quantitative morphometric data obtained from the indirect implants. Groups were: Heparin treated (Hep) and PGG followed by Heparin (PGG, Hep) treated ETVGs. IEL diameter, wall thickness, elastin and lumen area are shown. Representative images of (G) Masson trichrome stain and (H) CD31 stain for blood vessels; bar is 50 mm. AC, adventitial capsule; G, initial graft. Lumen is at left in both images. (For interpretation of the references to color in this figure legend, the reader is referred to the web version of this article.)

the hypothesis that xenogeneic matrices, if well decellularized, can serve as excellent tissue scaffolds [33,34].

Graft encapsulation occurred irrespective of the graft pretreatment, indicating that stabilization of collagen and elastin does not prevent cell infiltration in the adventitia. While the adventitia was extensively repopulated with host cells and capillaries, few cells were found within the media of the implanted grafts. The mechanisms underlying this phenomenon are not known at this point, but it is possible that the compact IEL and adventitial elastin fibers averted cell infiltration from the lumen and adventitial sides, respectively.

Another major finding was the omnipresence of neo-intimal tissue which grew in thickness with time, remodeled and in some instances calcified. The neo-intima, potentially derived from transanastomotic tissue overgrowth [15,35] was covered by endothelium and thus was non-thrombogenic if intact; however, in few cases the neo-intimal tissue appeared disturbed, activated and associated with local thrombi. In all samples analyzed calcification was absent from the scaffold graft wall, denoting the fact that decellularized arteries are less prone to calcification in this model. Several aspects were noted to depend on the scaffold pretreatment. Only non-stabilized grafts exhibited dilatation, associated with visible elastin degeneration in vivo, specifically the IEL and the adventitial elastin fibers. PGG treatment as well as the heparinization crosslinking procedure both reduced elastin degeneration and the combination of the two was very effective in maintaining matrix integrity, pointing to stabilized arterial scaffolds as viable small diameter vascular grafts.

Overall, this is an accepted screening model for vascular grafts with the caveat that the grafts were relatively short and thus were most likely endothelialized intra-luminally by trans-anastomotic tissue overgrowth. Because of this phenomenon, it was difficult to assess the intrinsic thrombogenicity of the graft material; thus we pursued a second set of implants where the trans-anastomotic tissue overgrowth was avoided by separating the grafts from the anastomoses by two low porosity ePTFE segments (isolation-loop model or indirect grafts) with follow-up at 12 weeks as described recently [15,35]. When compared to the direct grafts these were covered by same collagenous vascularized tissue. However, by contradistinction to direct implants, the indirect grafts lacked neointimal tissue overgrowth with absence of thrombi. These results

highlight the fact that the exposed sub-endothelial basement membrane of acellular arteries (derived from removal of the endothelium during decellularization) was essentially nonthrombogenic in this animal model.

All together, these results provide data which allow us to speculate on the outcome of clinically applicable lengths of stabilized arterial grafts as viable small diameter vascular grafts. Since in most clinical applications, segments of at least 8-10 cm long would be implanted, we expect the proximal and distal peri-anastomotic regions of the ETVGs to behave similar to the direct implants described in this paper and the midway section of the graft, at least 3-4 cm away from the anastomosis, to behave similar to the indirect implants. Currently we are testing >10 cm-long, chemically stabilized small diameter ETVGs in sheep as carotid interposition grafts.

Finally, we recommend that the optimal approach to pre-clinical testing of potential materials to be used as small diameter vascular grafts should include the following steps. If the material is biologically derived, one should first perform adequate quality controls to ensure complete decellularization as well as preservation of the major extracellular matrix components, including DNA analysis, extensive histology and a-Gal analysis. Biologic or synthetic materials of about 2.5 mm in diameter and 10 mm length could be then tested by: 1) evaluating mechanical properties, including suture retention strength, burst pressure and compliance, 2) implanting samples subdermally in rats for initial biocompatibility, as described before [21], 3) testing tubular grafts as direct vascular graft implants to evaluate peri-anastomotic reactions, 4) testing as indirect isolation-loop implants to asses host reactions away from the anastomosis and 5) implant as >10 cm long grafts in large animals for pre-clinical validation.

Conclusions

In the current study, we show that gentle decellularization of porcine muscular arteries generated implantable nonimmunogenic small diameter ETVGs endowed with adequate mechanical properties and lack of susceptibility towards calcification. To increase stability in vivo, we chemically treated the elastin component with PGG and the collagen component with carbodiimide/heparin. Implantation of ETVGs as vascular grafts in rats resulted in high patency and animal survival, possibly due to the ubiquitous encapsulation of the grafts

within a stable vascularized collagenous capsule and to the lack of thrombogenicity of the exposed sub-endothelial basement membrane. Peri-anastomotic neo-intimal tissue overgrowth was a normal occurrence in direct implants; however this reaction was circumvented in indirect, isolation-loop implants. Implantation of non-stabilized ETVGs exhibited marked graft dilatation and elastin degeneration; however chemical stabilization of grafts significantly reduced elastin degradation and prevented aneurismal dilatation of vascular grafts in vivo without altering formation of the external capsule. Due to their resistance to thrombosis, dilatation and calcification, stabilized acellular arteries are promising candidates as small diameter vascular grafts.

Disclosure statement

The authors have no competing financial interests.

Acknowledgments

The authors wish to acknowledge the excellent technical support of Helen Ilsley and Anel Oosthuysen from UCT and the NIH Fogarty International Research Collaboration Research Award (FIRCA, R03 TW008941) to DS.

References

[1] Faries PL, Logerfo FW, Arora S, Pulling MC, Rohan DI, Akbari CM, et al. Arm vein conduit is superior to composite prosthetic-autogenous grafts in lower extremity revascularization. J Vasc Surg 2000;31:1119e27.

[2] . Cryopreserved saphenous vein allografts in infrainguinal revascularization: analysis of 240 grafts. J Vasc Surg 2003;38:15e21.

[3] Zehr BP, Niblick CJ, Downey H, Ladowski JS. Limb salvage with CryoVein cadaver

saphenous vein allografts used for peripheral arterial bypass: role of blood compatibility. Ann Vasc Surg 2011;25:177e81.

[4] Brewster DC. Current controversies in the management of aortoiliac occlusive disease. J Vasc Surg 1997;25:365e79.

[5] Klinkert P, Post PN, Breslau PJ, van Bockel JH. Saphenous vein versus PTFE for above-knee femoropopliteal bypass. A review of the literature. Eur J Vasc Endovasc Surg 2004;27:357e62.

[6] Kurobe H, Maxfi. Stem Cells Transl Med 2012;1:566e71.

[7] Huang AH, Niklason LE. Engineering of arteries in vitro. Cell Mol Life Sci; 2014. http://dx.doi.org/10.1007/s00018-013-1546-3.

[8] Klopsch C, Steinhoff G. Tissue-engineered devices in cardiovascular surgery. Eur Surg Res 2012;49:44e52.

[9] neering: the next generation. Trends Mol Med 2012;18:394e404.

[10] Chow JP, Simionescu DT, Warner H, Wang B, Patnaik SS, Liao J, et al. Mitigation of diabetes-related complications in implanted collagen and elastin scaffolds using matrix-binding polyphenol. Biomaterials 2013;34:685e95.

322*T. Pennel et al. / Biomaterials 35 (2014) 6311e6322*

[11] Tedder ME, Liao J, Weed B, Stabler C, Zhang H, Simionescu A, et al. Stabilized collagen scaffolds for heart valve tissue engineering. Tissue Eng A 2009;15: 1257e68.

[12] ment with tannic acid. Biomaterials 2004;25:3293e302.

[13] patibility and remodeling potential of pure arterial elastin and collagen scaffolds. Biomaterials 2006;27:702e13.

[14] Lu Q, Ganesan K, Simionescu DT, Vyavahare NR. Novel porous aortic elastin and collagen scaffolds for tissue engineering. Biomaterials 2004;25: 5227e37.

[15] graft model. J Vasc Surg 2013;58:1053e61.

[16] Tai NRM, Giudiceandrea A, Salacinski HJ, Seifalian AM, Hamilton G. In vivo femoropopliteal arterial wall compliance in subjects with and without lower limb vascular disease. J Vasc Surg 1999;30:936e45.

[17] Riesenfeld J, Roden L. Quantitative analysis of N-sulfated, N-acetylated, and saccharides. Anal Biochem 1990;188:383e9.

[18] Bezuidenhout D, Davies N, Black M, Schmidt C, Oosthuysen A, Zilla P. Covalent tion. J Biomater Appl 2010;24:401e18.

[19] Bezuidenhout D, Oosthuysen A, Human P, Weissenstein C, Zilla P. The effects extended glutaraldehyde-fitechnol Appl Biochem 2009;54:133e40.

[20] Beckstead JH. A simple technique for preservation of figens in paraffin-embedded tissues. J Histochem Cytochem 1994;42:1127e34.

[21] Chuang TH, Stabler C, Simionescu A, Simionescu DT. Polyphenol-stabilized tubular elastin scaffolds for tissue engineered vascular grafts. Tissue Eng A 2009;15:2837e51.

[22] Mercuri JJ, Patnaik S, Dion G, Gill SS, Liao J, Simionescu DT. Regenerative potential of decellularized porcine nucleus pulposus hydrogel scaffolds: stem cell differentiation, matrix remodeling, and biocompatibility studies. Tissue Eng A 2013;19:952e66.

[23] Wu W, Allen R, Gao J, Wang YD. Artifinuclear cells. Tissue Eng A 2011;17:1979e92.

[24] . Tissue-engineered vascular grafts demonstrate evidence of growth and development when implanted in a juvenile animal model. Ann Surg 2008;248:370e7.

[25] . Characterization of the natural history of extracellular matrix production in tissue-engineered vascular grafts during neovessel formation. Cells Tissues Organs 2012;195:60e72.

[26] Isenburg JC, Karamchandani NV, Simionescu DT, Vyavahare NR. Structural . Biomaterials 2006;27:3645e51.

[27] Isenburg JC, Simionescu DT, Starcher BC, Vyavahare NR. Elastin stabilization for treatment of abdominal aortic aneurysms. Circulation 2007;115:1729e37.

[28] Zhang J, Li L, Kim SH, Hagerman AE, Lu J. Anti-cancer, anti-diabetic and other pharmacologic and biological activities of penta-galloyl-glucose. Pharm Res 2009;26:2066e80.

[29] Sierad LN, Simionescu A, Albers C, Chen J, Maivelett J, Tedder ME, et al. Design and testing of a pulsatile conditioning system for dynamic endothelialization of polyphenol-stabilized tissue engineered heart valves. Cardiovasc Eng Technol 2010;1:138e53.

[30] . Dog peritoneal and pleural cavities as bioreactors to grow autologous vascular grafts. J Vasc Surg 2004;39:859e67.

[31] cipient's own peritoneal cavity. Circ Res 1999;85:1173e8.

[32] Hayashida K, Kanda K, Yaku H, Ando J, Nakayama Y. Development of an in vivo tissue-engineered, autologous heart valve (the biovalve): preparation of a prototype model. J Thorac Cardiovasc Surg 2007;134:152e9.

[33] Crapo PM, Gilbert TW, Badylak SF. An overview of tissue and whole organ decellularization processes. Biomaterials 2011;32:3233e43.

[34] fold material: structure and function. Acta Biomater 2009;5:1e13.

[35] Zilla P, Bezuidenhout D, Human P. Prosthetic vascular grafts: wrong models, wrong questions and no healing. Biomaterials 2007;28:5009e27.

Section III

Conclusions and Future Directions

z

Decades of research into synthetic small-diameter vascular grafts has resulted in little progress beyond surface modifications and minor design changes of pre-existing polymers (ePTFE, PET). Recent exploration into tissue decellularization has shown relatives success in the laboratory, without clinicalyl relevant application. This lack of translation is due to limited understanding of the *in vivo* healing mechanisms. This study uses a three-stage screening assessment to determine *in vivo* healing of decellularized xenografts.

Although we have previously shown that alkaline decellularization of carotid arteries removes all cells and some of the collagen, this technique had not been applied to muscular arteries. We chose porcine renal arteries as the tissue source in this study in order to generate a size-matched xenograft for abdominal aortic implants in rats. It was demonstrated that the alkaline decellularization method was effective, with complete cell removal and the absence of the powerful xeno-antigen throughout the tissues.

The preservation of major tissue components (elastin and collagen) in their original configuration ensured adequate mechanical properties. Our results showed that suture retention strength, handling properties and burst pressures were unaltered by decellularization, while compliance values were reduced by about 50% as compared to fresh arteries. These results suggest that load-bearing structural components were well preserved, while other elements responsible for recoil (elastin associated microfibrils, proteoglycans) were probably removed by decellularization.

Although the majority of researchers' report on 'bench' as well as direct implant *in vivo* models, we believe that the short length used in these animal models have limited clinical translation. As was shown in this study, an endothelialized surface in a straight interposition graft in the infra-renal rat of the aorta could not be replicated when isolating the graft from the anastomosis. This is particularly relevant to human implant as the lack of endothelialization beyond the anastomosis has been well documented even after eleven years of implant[80]. It is of our opinion that anastomotic isolation models are essential for translating mid-graft healing to human implants.

It is clear that all endothelialization described in this study occurred through transanastomotic means, confirmed by the lack of endothelium seen on the isolated grafts. However, the high patency and lack of

mural thrombus highlight the fact that the exposed sub-endothelial basement membrane of acellular arteries (derived from removal of the endothelium during decellularization) was essentially non- thrombogenic in this animal model. Although these results should be interpreted with caution due to the inherent forgiving thrombogenicity of rats, the internal elastic lamina may represent a sufficiently non-thromobgenic which may require an endothelial layer for long term patency, a feature which would have significant impact for human implant.

Although the rat serves as an excellent screening tool, not only are porcine and ovine models a pre-clinical requirement for the FDA, but the implantation of longer (clinically relevant) conduit lengths is the next logical step. The highly muscular renal artery xenograft, although well suited to the infra renal rat aorta, served only as a proof of concept and would have little translational value to the treatment of PAD. The abundance of segmental branches within the renal artery is convenient for selecting the appropriate size for implant in the infra renal rat aorta, however the length of each segment is limited to 20mm, negating its use for clinical relevant implant.

We have already shown in our laboratory (unpublished data) that native bovine and femoral arteries could be fully decellularized, which would provide sufficient length of an infra-inguinal bypass graft in humans. The mechanical properties exceed the criteria necessary for functional arteries and their limited muscular layer may be more conducive to transmural healing although this is speculative. It is thus proposed that future research should include a large animal (ovine/porcine) model, with preference to the infra-inguinal position, although the carotid artery could be considered as an intermediate step due to its favorable flow dynamics.

Ultimately the goal is a human implant and the conduit used in the large animal model should be carefully considered for this purpose. There are only a few alternatives for small-diameter conduits of adequate length, such as human umbilical and cadaveric femoral vessels. However, we believe that the tapering nature of the bovine mammary artery may be advantageous with a technically easier proximal anastomosis as well as size matched distal anastomosis negating anastomotic size mismatch. Future experimental work on these theoretical properties would be required.

In conclusion, the implantation of non-stabilized decellularized arteries in this study exhibited marked graft dilatation and elastin degeneration; however chemical stabilization of grafts significantly reduced elastin degradation and prevented aneurismal dilatation of vascular grafts in vivo without altering formation of the external capsule. Due to their resistance to thrombosis, dilatation and calcification, stabilized acellular arteries have been shown to be promising candidates as small diameter vascular grafts through a three-stage screening model.

Section III

Published Manuscript

Biomaterials 35 (2014) 6311–6322

Contents lists available at ScienceDirect

Biomaterials

journal homepage: www.elsevier.com/locate/biomaterials

The performance of cross-linked acellular arterial scaffolds as vascular grafts; pre-clinical testing in direct and isolation loop circulatory models

Timothy Pennel [a], George Fercana [b], Deon Bezuidenhout [a], Agneta Simionescu [b], Ting-Hsien Chuang [b], Peter Zilla [a], Dan Simionescu [b,*]

[a] Christian Barnard Department of Cardiothoracic Surgery, Cardiovascular Research Unit, University of Cape Town, Faculty of Health Sciences, Cape Heart Center, Chris Barnard Building, Anzio Road, ZA 7925 Observatory, Cape Town, South Africa
[b] Biocompatibility and Tissue Regeneration Laboratories, Department of Bioengineering, Clemson University, Clemson, SC, USA

ARTICLE INFO

Article history:
Received 14 March 2014
Accepted 16 April 2014
Available online 9 May 2014

Keywords:
Thrombogenicity
Scaffolds
Elastin
Collagen
Dilatation
Degeneration

ABSTRACT

There is a significant need for small diameter vascular grafts to be used in peripheral vascular surgery; however autologous grafts are not always available, synthetic grafts perform poorly and allografts and xenografts degenerate, dilate and calcify after implantation. We hypothesized that chemical stabilization of acellular xenogenic arteries would generate off-the-shelf grafts resistant to thrombosis, dilatation and calcification. To test this hypothesis, we decellularized porcine renal arteries, stabilized elastin with penta-galloyl glucose and collagen with carbodiimide/activated heparin and implanted them as transposition grafts in the abdominal aorta of rats as direct implants and separately as indirect, isolation-loop implants. All implants resulted in high patency and animal survival rates, ubiquitous encapsulation within a vascularized collagenous capsule, and exhibited lack of lumen thrombogenicity and no graft wall calcification. Peri-anastomotic neo-intimal tissue overgrowth was a normal occurrence in direct implants; however this reaction was circumvented in indirect implants. Notably, implantation of non-treated control scaffolds exhibited marked graft dilatation and elastin degeneration; however PGG significantly reduced elastin degradation and prevented aneurismal dilatation of vascular grafts. Overall these results point to the outstanding potential of crosslinked arterial scaffolds as small diameter vascular grafts.

Published by Elsevier Ltd.

1. Introduction

Almost 1.4 million vascular grafts are needed every year in the US alone to replace diseased arteries. Of these, about 200,000 are small and medium diameter grafts (4–6 mm) for vascular access and to relieve lower limb ischemia and more than 600,000 are small diameter grafts (1–4 mm) needed for coronary bypass procedures. The conduit of choice for small diameter vascular graft surgery is the autologous vein or artery, but these are not available in 25–30% of patients due to preexisting conditions or previous harvesting [1]. Current grafts are made of polyethylene terephtalate (Dacron) or expanded polytetrafluoroethylene (ePTFE), or biologically derived conduits such as cryopreserved saphenous vein allografts and decellularized bovine ureters [2,3]. Synthetic grafts are being used successfully for replacements of large caliber arteries (above 8 mm internal diameter) with acceptable long term patency [4]. However when the same materials are used in small diameter applications (less than 6 mm internal diameter), they perform very poorly as peripheral arteries, with 50% of them occluding within 5 years, potentially leading to amputation. This is due to the intrinsic thrombogenicity of the materials, significant compliance mismatch leading to peri-anastomotic intimal hyperplasia and lack of remodeling and growth when implanted in young patients [5]. Short term results of biological grafts are also quite promising, but despite their “off the shelf” appeal, poor 1-year patency, extended thrombosis, aneurysmal degeneration leading to rupture and calcification have limited the use of such conduits [6]. This daunting lack of options has prompted surgeons to implant small diameter vascular grafts made of synthetic polymers with suboptimal results.

Therefore, surgeons welcome the possibility of gaining access to “off-the-shelf” small diameter grafts that would be easy to suture,

* Corresponding author. Department of Bioengineering, Clemson University, 304 Rhodes Annex, Clemson, SC 29634, USA. Tel.: +1 864 656 5559; fax: +1 865 656 4466.
E-mail address: dsimion@clemson.edu (D. Simionescu).

http://dx.doi.org/10.1016/j.biomaterials.2014.04.062
0142-9612/Published by Elsevier Ltd.

exhibit adequate compliance and burst pressures, remain patent and resist thrombosis and be resistant to aneurismal degeneration and calcification. It is believed that tissue engineering has the potential to generate such viable grafts by combining synthetic or naturally derived degradable or non-degradable scaffolds with a variety of cells followed by maturation in bioreactors. Such constructs have been tested in animal models but few of them have reached clinical trials because of their tendency to degenerate, dilate and calcify after implantation [6–9].

To overcome aneurismal degeneration and dilatation, we hypothesized that superior vascular graft scaffolds can be produced by chemically stabilizing acellular arteries. To test this hypothesis, we pioneered the use of elastin-rich tubular vascular grafts (ETVGs) produced from porcine arteries from which all cells and most of the collagen has been selectively removed. This approach has the advantage of creating a 3-D porous structure and maintaining native tissue architecture and arterial matrix "niche" while removing xeno-antigens. We were also the first to describe treatment with pentagalloylglucose (PGG) an elastin-stabilizing polyphenolic tannin to reduce biodegradation and calcification of ETVGs [10–12]. In addition we showed that PGG-treated ETVGs exhibited adequate mechanical and biological properties in vivo by subdermal implantation and were non-thrombogenic in acute implantation studies in rabbits [13,14]; recently we also showed that PGG treatment diminished the tendency of ETVGs to undergo diabetes-related alterations in vivo [10] which could become relevant if these grafts will be implanted in diabetic patients. Encouraged by these results, we are now for the first time presenting data regarding pre-clinical testing of stabilized ETVG grafts in a circulatory model in the rat using direct implantation as transposition grafts with 4 and 8 week follow up and indirect implantation using the isolation-loop approach with 12 week follow-up, a recently validated approach as a high throughput model for testing mechanisms of endothelialization [15].

2. Materials and methods

2.1. ETVG preparation, stabilization and characterization

Fresh porcine kidneys were obtained from the local abattoir and stored on ice while in transit back to the laboratory. The interstitial renal arteries (2.5–3.5 mm diameter, 10–15 mm length) were dissected, cleaned and decellularized by an alkaline treatment (0.1 M NaOH at 37 °C for 3 h). Scaffolds were extensively rinsed with sterile ddH_2O until the pH of rinse solutions dropped to about 8 and then finally rinsed in sterile PBS. Batches of scaffolds were further treated with sterile 0.1% pentagalloylglucose (PGG, Omnichem Ajinomoto, Belgium) in 50 mM phosphate buffer pH 5.5 containing 20% isopropanol for 24 h, rinsed and stored in sterile PBS. After sterilization for 24 h in 0.1% peracetic acid in sterile PBS, scaffolds were rinsed in sterile PBS and stored at 4 °C for up to 3 months. Scaffold decellularization efficacy was qualitatively assessed by histology using DAPI nuclear staining and Hematoxylin–Eosin (H&E) for cell nuclei and general matrix morphology, Masson's trichrome for collagen and smooth muscle proteins and Voerhoff van Gieson (VVG) stain for elastin and biotinylated GS lectin histochemistry for α-Gal [11]. DNA was also extracted from fresh arterial tissue and decellularized scaffolds using a Qiagen extraction kit and samples analyzed by PicoGreen assay and by ethidium bromide agarose gel electrophoresis.

2.2. Mechanical properties

For measurement of suture retention strength, ETVG samples were cut into 5 × 10 mm segments ($n = 6$ per group) and one end was clamped to an 10 N MTS test frame (MTS Systems Corp., Eden Prairie, MN). A single 4-0 braided suture was placed 1 mm from the free edge and its end tied to the MTS test frame. Samples were then preloaded to 0.005 N and extended to failure at 5 mm/min; final data was expressed as grams-force.

For compliance and burst pressure analysis, ETVGs ($n = 6$ per group) were adapted on both ends with barbed Luer connectors and secured with a clamp at each connector. A peristaltic pump was used to progressively fill sections with PBS at room temperature and a pressure transducer was mounted on the distal end of the arterial scaffold to record pressures continuously via a computer interface. For diametrical compliance, segments were exposed to 80 mmHg and 120 mmHg and digital images were captured at each pressure setting. The images were then imported into SolidWorks and mean outside diameter calculated digitally using measurements at 6 positions perpendicular to the ETVG sides. Diametrical compliance was then calculated using equations published by Hamilton's group [16]. A similar setup was used to assess burst pressures ($n = 6$ per group) using the peristaltic pump to progressively fill sections with PBS until rupture.

2.3. Scaffold heparinization

To optimize the heparinization protocol, PGG and non-PGG treated ETVG samples were rinsed in phosphate buffered saline (PBS), reacted with Jeffamine, amine-terminated polypropylene glycol, (Huntsman) 240 mM in 0.25 M MES buffer, pH = 5, 2 h at room temperature using a combination of 1-Ethyl-3-(3-dimethylaminopropyl) carbodiimide and N-hydroxysuccimimide (EDC/NHS, 300/10 mM) as activator. After another PBS rinse, nitrous acid degraded heparin (Celsus; 2 mg/ml; in 0.15 M NaCl; pH = 3.9, solution containing 1 mg/ml $NaCNBH_3$) was coupled by reductive amination to the aminated and non-aminated control samples by a 16 h reaction at room temperature. The treatments were performed either with or without pre-soaking in Heparin and samples were subsequently rinsed and stored in sterile PBS.

2.4. Heparin quantification

The heparin content of ETVGs ($n = 3$) was quantitatively determined by 3-methyl-2-benzothiazoninone hydrazone (MBTH) assay adapted from Risenfeld and Roden [17] similar to that described before by Bezuidenhout et al. [18]. Heparin content (mg/g tissue) was calculated from standard curves.

2.5. Heparinization of grafts for implantation

Heparinized ETVG samples for implantation were prepared as described above via Jeffamine functionalization (without pre-soaking) and heparin attachment using 0.2 μm-filtered solutions under sterile conditions in a laminar flow hood. The following four implant groups were thus generated: 1) untreated (None); 2) PGG-treated (PGG); 3) Heparin (Hep); and 4) PGG followed by Heparin (PGG, Hep).

2.6. Denaturation temperature determination

Thermograms of ETVG samples (5–10 mg, $n = 3$) in sealed aluminum sample pans were obtained at a heating rate of 10 °C/min (DSC 7; Perkin Elmer) and the onset temperature of the denaturation endotherm recorded as the denaturation temperature [19].

2.7. Resistance to enzymatic degradation

ETVG samples ($n = 6$ per group and per enzyme) of about 3 × 3 mm were lyophilized and their masses recorded to obtain dry tissue mass. For collagenase resistance, samples were incubated in 1 ml solution of 20 units/mL ultrapure type VII collagenase (Sigma) in 1 mM $CaCl_2$ 100 mM Tris (hydroxymethyl) aminomethane at pH 7.8 and 0.02% NaN_3. For elastase resistance, samples were incubated in 1 ml of 6.25 units/mL ultrapure elastase (Elastin Products Company) in the same buffer. After incubation at 37 °C for 24 h with mild agitation, samples were centrifuged at 12,000 RPM, rinsed three times with ddH_2O, lyophilized and weighed to calculate percent mass loss during enzyme digestion.

2.8. Implant groups

For direct implants, a total of 52 rats were implanted with vascular grafts to complete a targeted $n = 12$ per ETVG group, with $n = 6$ per time point. Three rats were replaced due to premature graft rupture at 6 weeks. For isolation-loop implantation, we first prepared two groups of 2.5–3 mm diameter, 10–15 mm long acellular grafts, namely Hep and PGG, Hep ($n = 6$ per group) as described above. Then we heat set 90 mm long low-porosity ePTFE segments for 3 min at 100 °C over a spiraled 1.5 mm nylon cord to generate a stable alpha-loop structure without kinking. A 10 mm midway segment was then removed from the ePTFE loop and replaced with a ETVG segment by end-to-end anastomosis with interrupted 9-0 nylon (Ethilon; Johnson & Johnson, New Brunswick, NJ) using an operating microscope (Zeiss Universal S3 OPMI 6-SFC, Oberkochen, Germany).

2.9. Graft implantation

All animal experiments were approved by the Animal Research and Ethics Committee of the University of Cape Town and were in compliance with the Guide for the Care and Use of Laboratory Animals, Institute of Laboratory Animal Resources, Commission on Life Sciences, National Research Council, South Africa. Male Wistar rats weighing 350–510 g were induced with isoflurane 5% anesthesia and were maintained with 2% isoflurane spontaneously breathing via a conical mask. Sterility was maintained throughout the procedure and a warming pad was used to regulate temperature. Following a mid-line laparotomy, the aorta was dissected free of the inferior vena cava and surrounding tissues and all perforating arteries between the left renal artery and the iliac bifurcation were ligated. In all cases the inferior mesenteric artery was preserved. A single dose of intravenous heparin (1 mg/kg) was administered and the direct grafts were implanted into the infrarenal aorta by end-to-end anastomoses using 9-0 Nylon interrupted sutures. The isolation-looped grafts were similarly implanted by anastomoses to the infrarenal

aorta and further secured with a suture to the lumbar muscles to prevent twisting. The abdomen was closed in layers and Buprenorphine (0.1 mg/kg) was administered subcutaneously twice daily for three days. No anticoagulation medication was administered after surgery.

2.10. Graft removal

Following 4 and 8 weeks for direct implants and 12 weeks for isolation-loop implants, the abdomen was opened and the grafts inspected for patency by observation of pulsation in the distal aorta, under general anesthesia as for the implant procedure. Animals were euthanized by exsanguination following 1 mg/kg heparin administration via the inferior vena cava. The aorta was flushed with phosphate-buffered solution via the apex of the left ventricle until clear of blood (cca.150 ml), following which the aorta was perfusion fixed with formalin. The graft was then excised, cross-sectioned for macro-photography and processed for histology.

2.11. Histology and quantification

Tissue samples were post fixed in zinc solution [20], dehydrated, embedded in paraffin, sectioned and processed for histological examination. Hematoxylin–Eosin and Miller and Masson's trichrome stain (ELMAS) were used for basic light histological analysis. Immunofluorescent identification of endothelial cells was performed with antibodies to Factor 8 (Dako), CD3 for lymphocytes (Dako), ED1 for pan-macrophages (Serotec), CCR7 for M1 macrophages (Abcam), ED2 for M2 macrophages (Serotec), alpha-smooth muscle cell actin (Dako), using Cy3 conjugated streptavidin or Alexa Fluor 488 GxR (Invitrogen). Immunohistochemistry for endothelium was also performed with anti-CD31 antibodies (Fitzgerald). Elastin and calcification was identified with Orcein and Alizarin red stain respectively, and glycosaminoglycans were stained with Alcian blue. Quantitative measurements of wall thickness, lumen area, internal elastic lamina (IEL) diameter and neo-intimal pannus overgrowth were performed on trichrome stained sections with Visiopharm Integrated Systems software (VIS, Visiopharm A/S, Hoersholm, Denmark) and Adobe Photoshop CS6 on mid-graft cross-sections.

2.12. Statistical analysis

Statistical tests were performed with STATA (StataCorp. 2011. *Stata Statistical Software: Release 11* College Station, TX: StataCorp LP) Results were expressed as mean ± SD for continuous variables. All continuous data was confirmed as nonparametric (Shipiro–Wilkinson) interrogated with Mann Whitney test for statistical significance. Kruskal–Wallis equality-of-populations rank test was used for multiple group analysis. Categorical data was tested with the Fishers exact, and the level of significance was set at $p < 0.05$. Burst pressures, diametrical compliance and enzyme resistance were compared using ANOVA, and effect of heparinization and denaturation temperatures with student's *t*-test.

3. Results

3.1. Scaffold preparation and characterization

To generate 2.5–3.5 mm diameter, 10–15 mm long vascular grafts, we dissected segmental and inter-lobar arteries from adult porcine kidneys and decellularized them with NaOH as reported previously with minor modifications [21]. Completeness of decellularization was confirmed lack of extractable DNA, absence of cell nuclei in histological DAPI staining (Fig. 1) and histological analysis including H&E, Trichrome, and α-Gal antigen lectin histochemistry, all of which depicted cells in native tissues and their absence in decellularized ETVGs. Acellular renal arteries showed good preservation of overall arterial matrix morphology including native collagen and elastin (Fig. 1). Notable histological features of the acellular renal arteries included a distinct internal elastic lamina (IEL), a relatively thin media containing thin elastin and collagen fibers and a very thick elastin and collagen-rich adventitia. Suture retention strengths and burst pressures of acellular arteries were not different from those of native arteries (Fig. 2). However, decellularization reduced diametrical compliance by about 50% (Fig. 2).

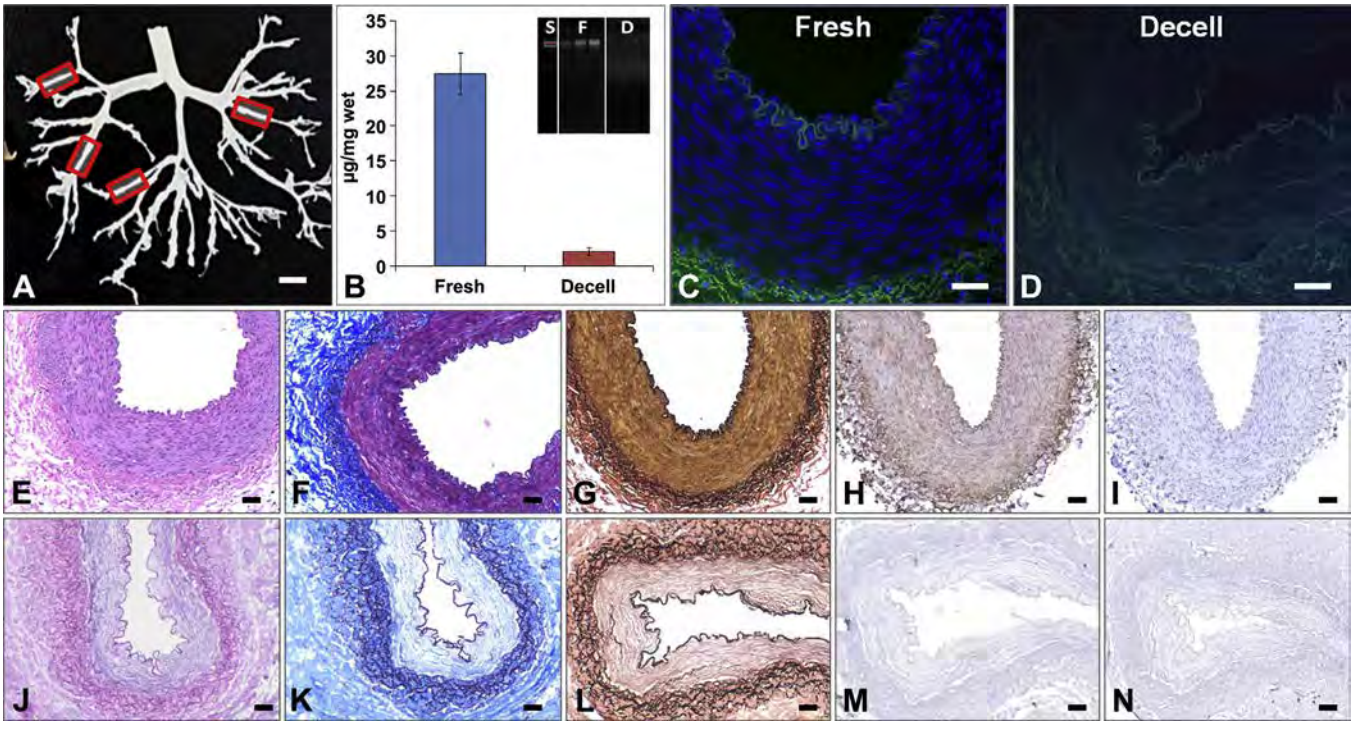

Fig. 1. Vascular scaffold data. (A) A whole porcine kidney arterial tree is shown after it was dissected and cleaned manually. Segmental and interlobar arteries (red squares) of 2–3 mm diameter and 10–15 mm length were dissected and decellularized as described in the manuscript. Bar is 10 mm. (B) DNA was extracted from fresh and decellularized (Decell) arteries and quantified using Picogreen (µg/mg, $n = 6$ samples per group) and verified with ethidium bromide agarose gel electrophoresis (insert, $n = 3$, S, DNA standard; F, fresh; D, decellularized). (C) DAPI nuclear stain (blue) superimposed over green elastin autofluorescence was used to highlight cells in fresh arteries and (D) lack of cells in decellularized (Decell) grafts. Images are representative for $n = 6$, bars are 50 µm. Lower panels show histology of fresh (E–H) and decellularized (J–M) arteries using H&E, (E, J), Masson's trichrome (F, K), Verhoeff van Gieson (G, L), and α-Gal histochemical detection using GS lectin (H, M). Images are representative for $n = 6$ per group, bars are 50 µm. (I, N) are α-Gal histochemistry negative controls for fresh and Decell, respectively. (For interpretation of the references to color in this figure legend, the reader is referred to the web version of this article.)

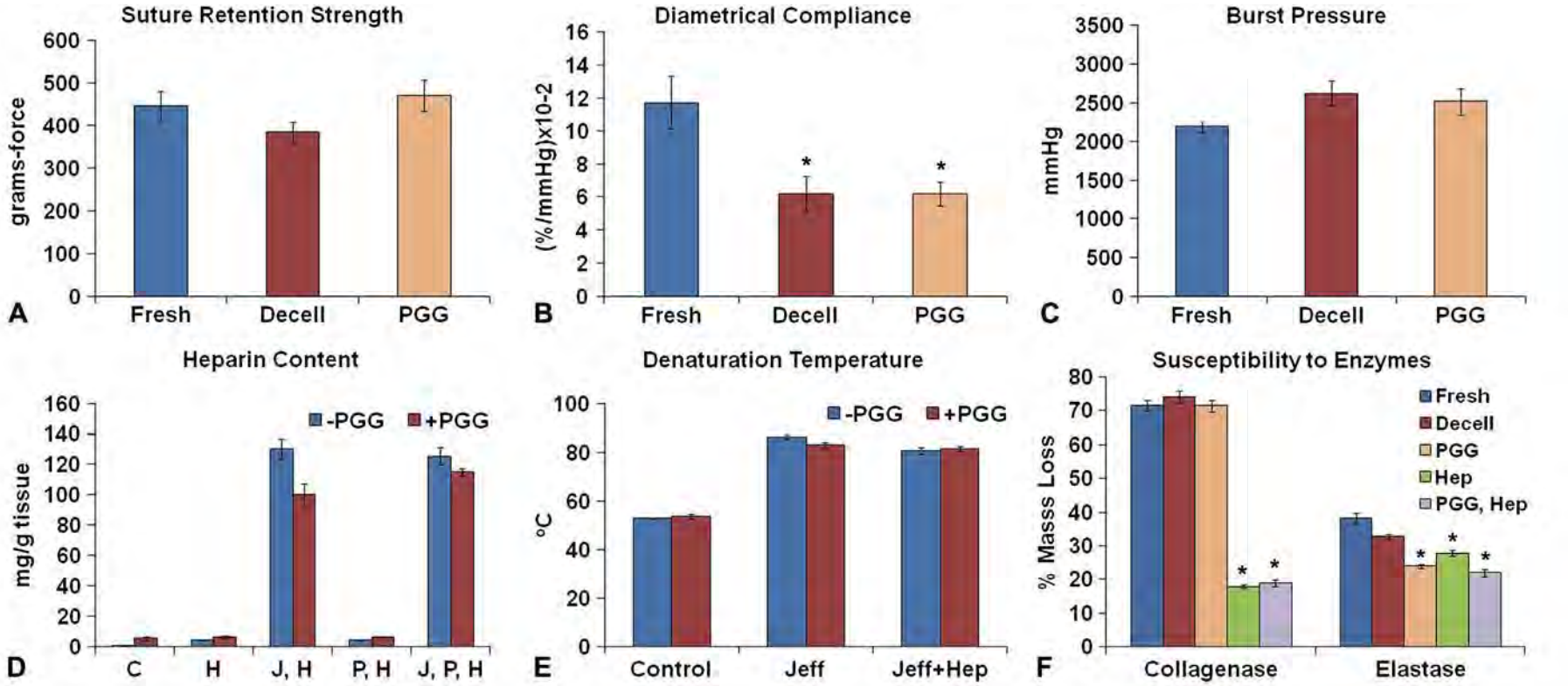

Fig. 2. Characterization and stabilization of acellular arterial scaffolds. (A) Suture retention strength, (B) diametrical compliance and (C) burst pressure values for fresh arteries, decellularized (Decell) arteries and PGG-treated Decell arteries (PGG). Data was obtained from $n = 6$. *-statistically significant as compared to fresh, $p < 0.05$. (D) Heparin content of untreated ETVGs (−PGG) and PGG treated scaffolds (+PGG). Groups were: Controls (C) not subjected to treatments, (H) treated with activated heparin alone and treated with Jeffamine (J) with and without pre-soaking in heparin (P). (E) Graft crosslinking as evaluated by DSC test for untreated (−PGG) and PGG treated samples (+PGG) before (Control) and after treatment with Jeffamine (Jeff) or Heparin (Hep), or Jeff followed by Hep (Jeff + Hep). (F) Five ETVG groups were prepared and tested for resistance to enzymes: fresh renal arteries, decellularized arteries (Decell), and Decell treated with PGG alone (PGG), Heparin alone (Hep), and PGG followed by Hep (PGG, Hep). $n = 6$ per group; *-statistically significant as compared to Decell, $p < 0.05$.

Table 1
Summary of direct grafts.

	4 w	8 w	Ruptured	Replaced	Survival at 4 w (%)	Survival at 8 w (%)	Excluded[a]	Analyzed
Non	6	8	2	2	85	92	2[b]	12
PGG	6	8	1	1	100	100	3[c] + 1[b]	10
Hep	6	6	0	0	100	100	1[c]	11
PGG, Hep	6	6	0	0	100	100	0	12

[a] Excluded from quantitative analysis:
[b] Ruptured grafts ($n = 3$).
[c] Grafts explanted at designated time points which exhibited outside diameter >3.5 mm and an aortic to graft diameter ratio <0.4 at implant.

3.2. Stabilization and heparinization

To increase biocompatibility, untreated and PGG-treated ETVGs were heparinized by covalent immobilization of nitrous acid activated heparin (which contains aldehyde end-groups for end-point attachment). To monitor efficacy, we measured heparin content in each group of tissues. Simple soaking in activated heparin did not result in heparin binding because acellular arteries did not contain sufficient exposed amine groups. Thus, we first aminated the ETVGs using diamines (Jeffamine) and carbodiimide chemistry. Control samples showed low baseline levels of heparin, irrespective of PGG treatment. No differences were seen between the tissue samples which were pre-soaked in heparin or not (Fig. 2). Significantly and much higher heparin content values were observed for samples that were first aminated with Jeffamine/carbodiimide prior to the reaction with heparin. PGG did not interfere with the reaction, and pre-soaking in heparin did not significantly affect the heparin content of ETVGs (Fig. 2). Jeffamine/carbodiimide treatment alone resulted in significant increases in denaturation temperature ($p < 0.001$) of the grafts (Fig. 2) indicative of crosslinking. Further reaction of aminated scaffolds with activated heparin did induce further chemical crosslinking in both −PGG or +PGG scaffolds. These results indicate that covalent immobilization of heparin cross-links the ETVGs and that PGG does not impede heparinization. Analysis of resistance to collagenase and elastase showed that decellularization did not significantly change tissue susceptibility to enzymes ($p > 0.05$). PGG treatment of ETVGs reduced their susceptibility to elastase by about 50% while heparinization stabilized collagen by more than 80% (Fig. 2), indicating that PGG stabilizes elastin while heparinization treatment cross-links collagen.

3.3. Direct implants; surgical handling and implants statistics

Although the surgeon was not blinded at the time of graft implant, surgical handling was adequate for all vascular grafts and subjectively superior in the heparinized set of grafts (Hep and PGG, Hep groups). The goal of this study was to ensure completion of $n = 6$ implants per time point per group. The implant statistics

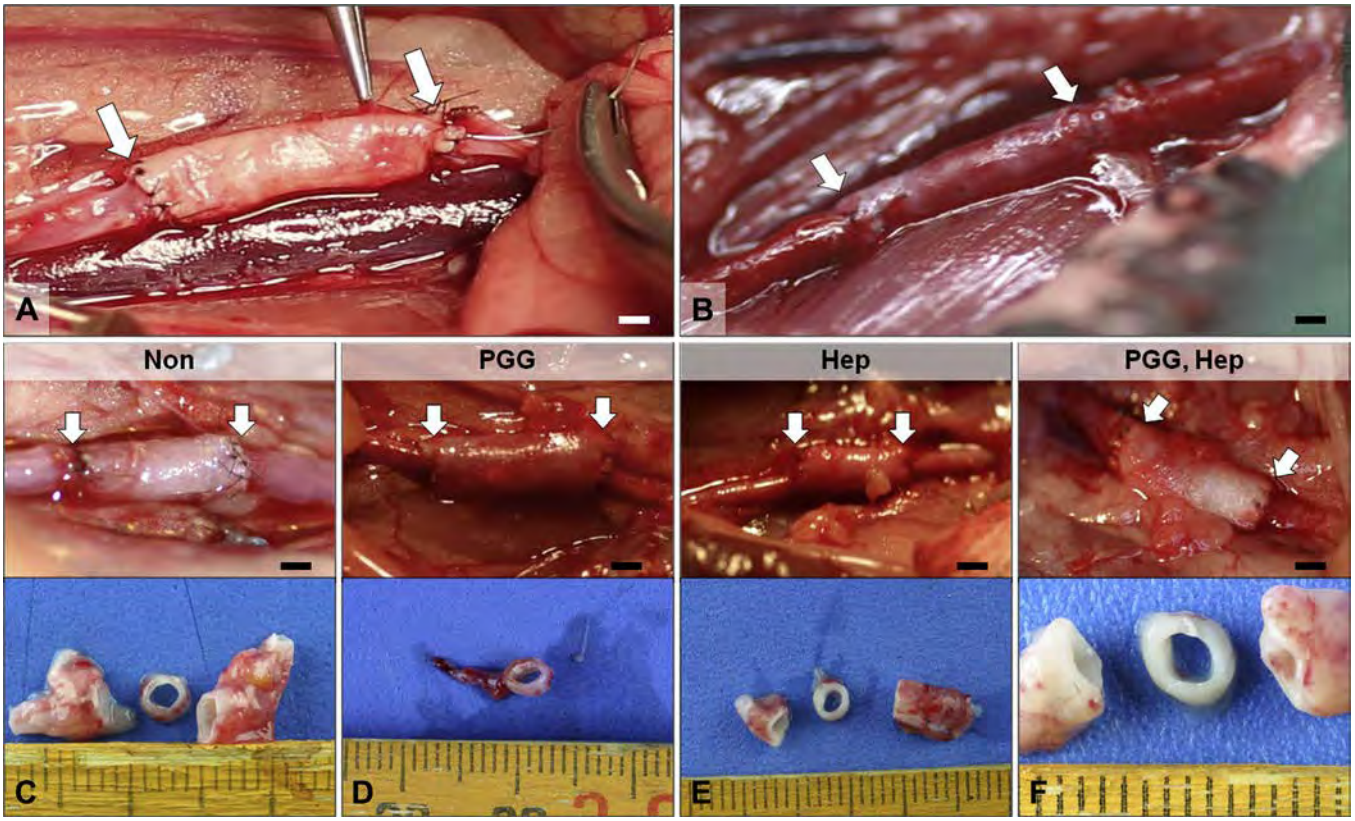

Fig. 3. Intra-circulatory implantation of ETVGs as direct grafts. (A–B) macroscopic images showing grafts during implantation in the rat infrarenal abdominal aorta; white arrows depict the anastomoses; bar is 1 mm. (C–F) representative macroscopic aspects of grafts before explantation (top) and macro images of midsections after perfusion fixation of corresponding grafts in each group (bottom). The groups were ETVGs without pre-treatment (Non) or treated with PGG alone (PGG), Heparin alone (Hep), and PGG followed by Hep (PGG, Hep). White arrows depict the anastomoses and bar in (C–F) is 1 mm.

(Table 1) show that only 3 grafts ruptured prior to their scheduled 8 week explant, all of which occurred after 6 weeks. Two of them were from the non-stabilized graft group ("Non") and one from the PGG-treated group. Rupture was confirmed at autopsy with abdominal blood and macroscopic evidence of wall defect. These grafts were subsequently replaced. After replacement, all of the animals survived to their designated explant time points and had 100% patent grafts (Table 1). An overview of implantation and explantation macroscopic aspects is shown in Fig. 3.

3.4. Direct implants; histological evaluation

All grafts, irrespective of the treatments they were subjected to, demonstrated concentric peri-graft tissue infiltration and formation of a well vascularized collagenous granulation tissue of about 600–800 μm in thickness (Fig. 4). Cells were seen infiltrating and completely re-populating the (initially acellular) graft adventitia without penetrating the media. This cellular infiltration was composed of CCR7-positive (M1) and ED2-positive (M2) macrophages, α-smooth muscle cell actin-positive myofibroblasts, foreign body giant cells and very few CD3-positive lymphocytes (Fig. 4). The thickness of this capsule did not increase from 4 to 8 weeks and did not appear to reduce the lumen diameter, suggesting little if any constrictive remodeling. A thin layer of neo-intimal tissue with the appearance of "intimal hyperplasia" but probably derived from peri-anastomotic pannus overgrowth, was also present in all direct implants. The neo-intimal tissue was rich in myofibroblasts and covered by a continuous layer of F8-positive endothelial cells (Fig. 4). In most explants analyzed, the neo-intimal tissue was stable and prevented formation of clots. However, in about 1/3 of all implants, irrespective of graft pre-treatment, the neo-intimal tissue underwent detachment or remodeling at 4 weeks, allowing for thrombus formation. At 8 weeks, the heparizined grafts (with or without PGG) did not exhibit any thrombus formation. Three neo-intima samples (out of total 45 analyzed) also exhibited chondroid metaplasia with Alcian Blue positive (not shown) and Alizarin Red positive structures (Fig. 4). Two additional samples stained positive for calcium in the neointima, in the absence of chondroid metaplasia. None of the acellular grafts showed any evidence of calcium deposition within the implanted graft wall.

To gather more quantitative data, we analyzed representative ELMAS-stained midway graft sections by digital morphometry and measured the perimeter of the IEL, wall area, lumen area, wall thickness and neo-intimal pannus area for each sample (Fig. 5). We also used Orcein stain for elastin and quantified the integrity of implanted elastin as a function of graft treatment.

When compared to pre-implant samples, the IEL diameter in all implanted grafts (irrespective of treatment) did not change after 4 weeks but increased significantly to almost 100% at 8 weeks in non-treated grafts (Fig. 6). The IEL diameters in grafts treated with PGG, Hep or PGG followed by Hep remained unchanged at 8 weeks ($p > 0.05$). Similarly, the luminal area was statistically larger only in the non-treated grafts at 8 weeks; grafts treated with PGG alone, Hep alone or PGG followed by Hep exhibited similar luminal areas

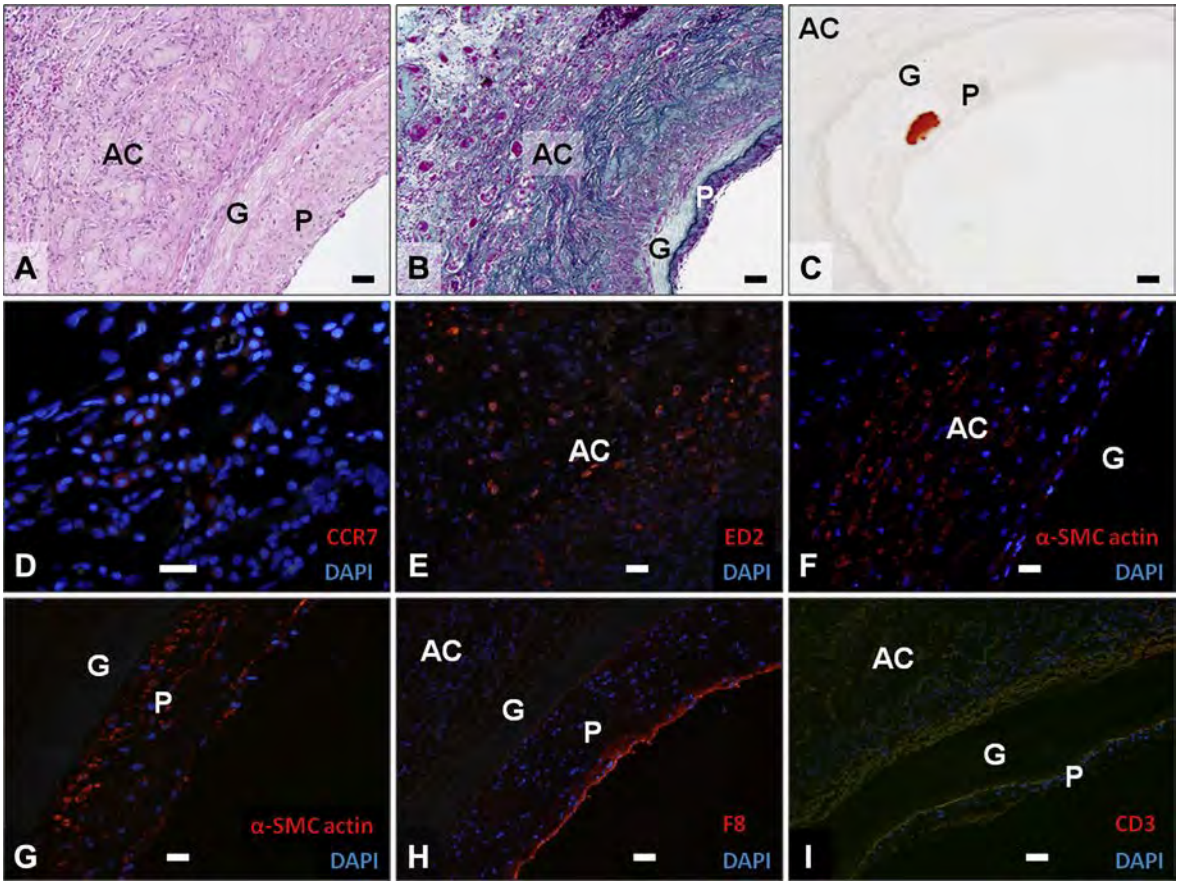

Fig. 4. Histology of explanted direct grafts. Representative sections shown after staining with (A) H&E, (B) Masson's trichrome, (C) Alizarin red, (D) CCR7 immunofluorescence (red) for M1 macrophages, (E) ED2 stain (red) for M2 macrophages, (F) α-smooth muscle cell actin (red) for activated myofibroblasts in the adventitia and (G) in the neo-intima; (H) F8 endothelial stain and (I) CD3 lymphocyte stain. (D–I) nuclei were counterstained with DAPI (blue); Images are representative for $n = 6$, bars are 50 μm. AC, adventitial capsule; G, initial graft; P, neo-intimal pannus. Lumen is at lower right in all images. (For interpretation of the references to color in this figure legend, the reader is referred to the web version of this article.)

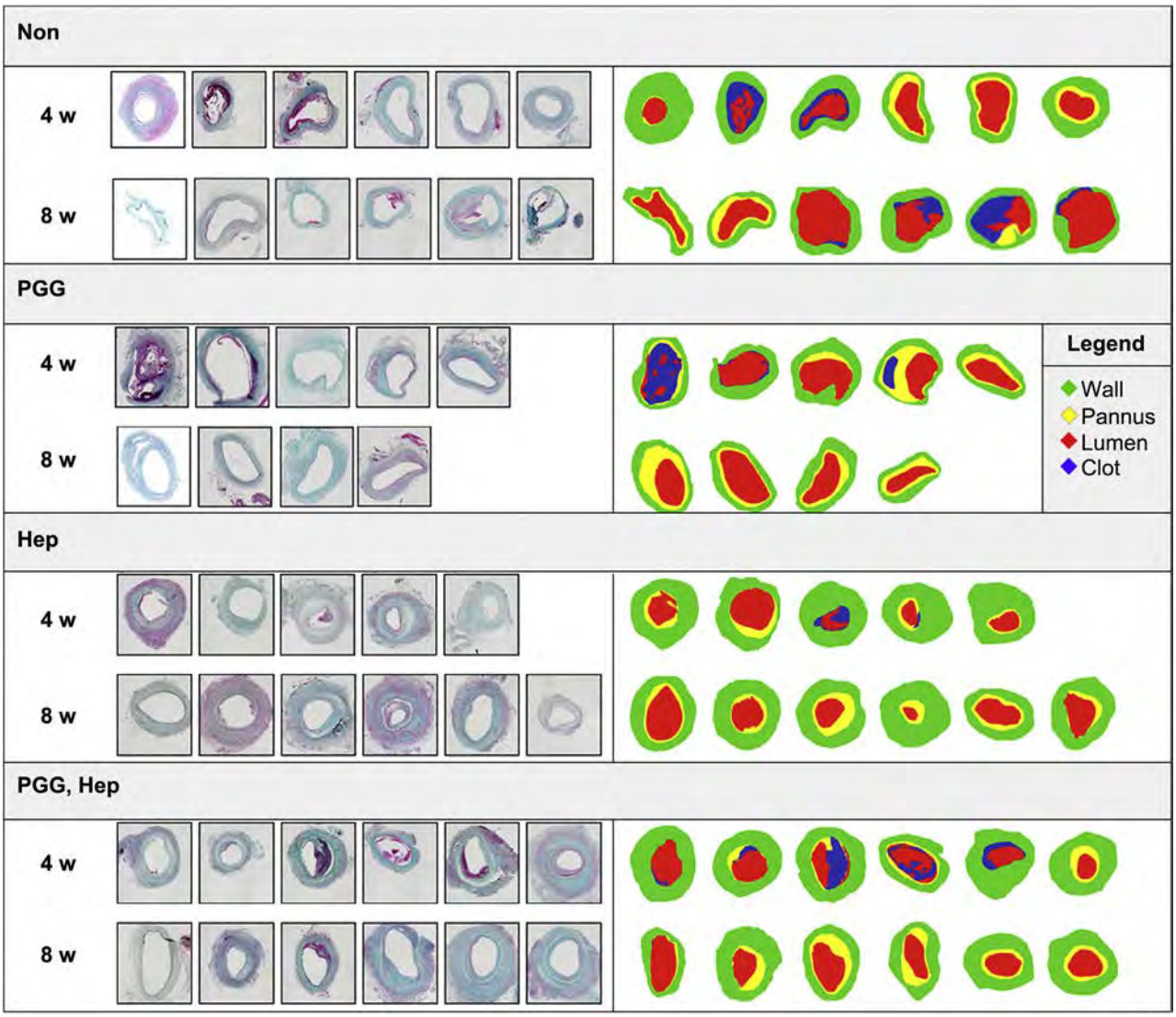

Fig. 5. Evaluation of explanted direct graft histology. Panel of representative Masson's stained mid-graft histology cross-sections from each individual implant retrieved at 4 weeks (4 w) and 8 weeks (8 w). ETVG groups were: untreated (Non), PGG-treated (PGG), Heparin treated (Hep) and PGG followed by Heparin (PGG, Hep). Histology images were digitized and color coded to measure wall thickness (green), pannus area (yellow), lumen area (red) and clot (blue). Stained sections are shown at left and corresponding digitized images at right. (For interpretation of the references to color in this figure legend, the reader is referred to the web version of this article.)

at 4 weeks without signs of progression at 8 weeks ($p > 0.05$). The graft wall thickness (collagenous granulation tissue) was similar in most groups (600–800 μm) except for PGG, where it was thinner ($p < 0.01$). Neo-intimal pannus thickness increased across all four groups from 4 weeks to 8 weeks as a result of peri-anastomotic tissue ingrowth (Fig. 6); however the differences among the four groups at 8 weeks were not statistically significant. Notably, statistically significant preservation of elastin with sequential stabilization treatments was measured in ETVGs (Fig. 6E). Both heparinization and PGG treatment independently resulted in a statistically significant improvement in elastin preservation (when compared to untreated controls) with an additive effect in their combination demonstrating that elastin, unless stabilized, is susceptible to in vivo degeneration. Elastin stabilization only correlated statistically to dilatation at 8 weeks (Bivariate Fit, $p = 0.0427$).

3.5. Evaluation of isolation-loop (indirect) implants

To test the hypothesis that the neo-intimal pannus observed in direct implants is related to trans-anastomotic tissue ingrowth and not to trans-mural cell infiltration, we sutured 10 mm-long graft segments midway in 9 cm long ePTFE loops such that the implanted grafts were 4 cm away from the anastomosis to the native abdominal artery (Table 2). The grafts were easy to suture onto the ePTFE material and they did not kink when forced into an alpha-loop configuration (Fig. 7). At explantation, the grafts were well integrated into host tissues, namely the retroperitoneum. In the Hep group 5/6 grafts were patent while in the PGG, Hep group 4/6 grafts were patent.

Similar to the direct implants, all isolation-loop grafts demonstrated formation of the external, well vascularized collagenous granulation tissue (Fig. 7). Quantitative morphometric comparisons between the two pre-treatments applied to the indirect grafts (Hep vs PGG, Hep) showed that there were no significant differences in wall (capsule) thickness, IEL diameter (dilatation), elastin preservation and lumen area ($p > 0.05$). Similarly, no statistical differences were noted in these four parameters when indirect implant data were compared to the direct implant results. The major differences between direct and indirect grafts were 1) the complete lack of neo-intimal pannus tissue formation in the isolation-loop

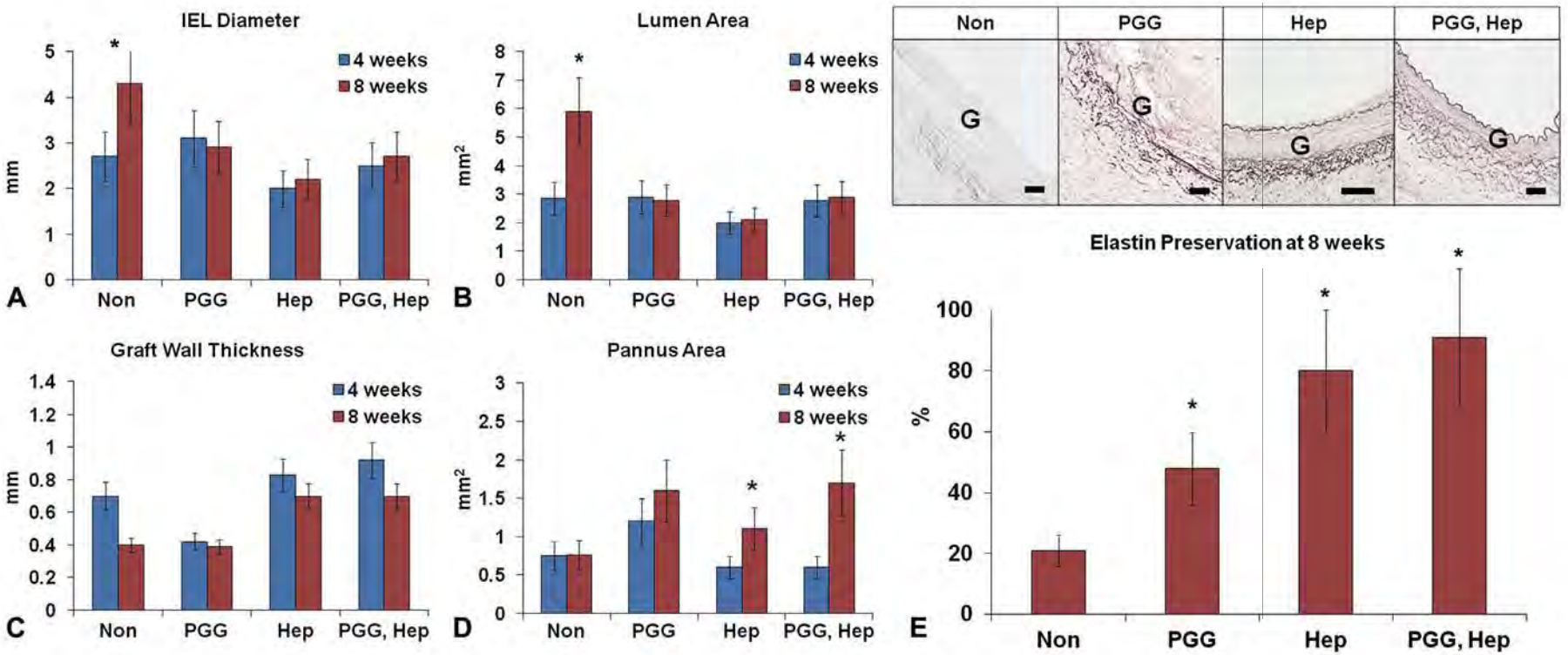

Fig. 6. Quantitative morphometric data obtained from direct implants. Digitized images (as shown in Fig. 5) were used to measure: (A) IEL diameter, (B) lumen area, (C) graft wall thickness and (D) pannus area in untreated ETVGs (Non), PGG-treated (PGG), Heparin treated (Hep) and PGG followed by Heparin (PGG, Hep). *-statistically significant as compared to 4 weeks, $p < 0.05$. (E) Orcein stain for elastin (top row) and quantification of elastin content from the histological images (bottom). *-statistically significant as compared to non-treated scaffolds (Non), $p < 0.05$. G, graft. Lumen is at top or top/right corner, bar is 50 μm.

Table 2
Summary for isolation-loop (indirect) grafts.

	Implanted	Ruptured	Patent	Analyzed
Hep	6	0	5	5
PGG, Hep	6	0	4	4

samples, irrespective of the graft pre-treatment and 2) significantly reduced thrombus formation. Since the arterial sub-endothelial basement membrane in the indirect grafts was not covered by pannus, this experiment also gave us the unique opportunity to evaluate the intrinsic thrombogenicity of the luminal surface of acellular arteries. As seen in the histology, immunofluorescence and SEM images, the surface of the 12 week indirect implants appeared wavy but relatively smooth and free of adhered cells, fibrin strands or microthrombi (Fig. 7).

4. Discussions

We have shown earlier that alkaline decellularization of carotid segments removes all cells and some of the collagen; however the NaOH technique was never applied to muscular arteries. Current results on renal arteries demonstrate that the alkaline decellularization method was effective, with complete cell removal as seen on DAPI stained sections and lack of extractable DNA, as well as lack of cells on histology stains (H&E, trichrome, VVG). Furthermore, acellular arteries lacked α-Gal staining which confirmed complete decellularization and also revealed the absence of the powerful xeno-antigen throughout the tissues.

We chose renal arteries as the tissue source in order to generate size-matched grafts which would be implanted into the abdominal artery of rats. In current studies we focused on acellular arteries as biological scaffolds for several reasons. First, because we believed that the biggest asset of acellular scaffolds prepared from target tissues is the presence of an architecturally accurate extracellular matrix network capable of presenting cell adhesion motifs for repopulation with differentiated cells as well as to serve as "niches" and cues for stem cell differentiation into desired cell types [22,23]. While cell removal reduced immunogenicity and generated pores allowing cell infiltration, it also raised concerns regarding the exposure of the vascular sub-endothelial layer to flowing blood. In current studies we showed that the sub-endothelial basement membrane of ETVGs was essentially non-thrombogenic. Second, preservation of major tissue components (elastin and collagen) in their original configuration ensured adequate mechanical properties. Our results showed that suture retention strength, handling properties and burst pressures were unaltered by decellularization, while compliance values were reduced by about 50% as compared to fresh arteries. These results suggest that load-bearing structural components were well preserved, while other elements responsible for recoil (elastin associated microfibrils, proteoglycans) were probably removed by decellularization. We and others have shown that among matrix components, the proteoglycans are rapidly lost during decellularization [14]. It remains to be determined whether these compliance levels (5–6%) will be important in the long run; however these values are similar to those reported by Hamilton's group for human femoral and popliteal arteries (4.7–6.1%) [16]. Third, maintenance of intact, mechanically functional elastin within the structure of scaffolds is a very important aspect of vascular tissue engineering. Elastin is almost impossible to incorporate into sheets or lamellae using a bottom–up approach and new mature elastin fibers are notoriously difficult to synthesize in vitro or in vivo [24,25]. Elastin is important for recoil properties of arterial tissues and thus its presence within our scaffolds may ensure extended mechanical durability. Moreover, elastin has a tendency to calcify and degenerate upon implantation and once lost in vivo, it will not likely be re-synthesized by resident or infiltrating cells. For this reason we used arteries as a starting material. After decellularization, elastin is evident in the form of a distinct layer in the IEL, as fine fibrils within the media and as an extensive 3D network of fibers within the adventitia. We then chose to treat ETVGs with PGG, an elastin binding polyphenol which reduces elastin's susceptibility to enzymatic degradation and also diminishes its calcification potential [11,21,26–29]. Recently we also showed that PGG treatment of elastin-rich scaffolds protected implants from diabetes-related glycation, crosslinking and alterations in mechanical properties, which might prove very beneficial for diabetic patients requiring peripheral vascular surgery [10].

Acellular arterial scaffolds derived from renal arteries also contained a significant amount of collagen specifically in the adventitia layer. In order to stabilize the collagen component and to increase implant hemocompatibility, we heparizined the scaffolds via carbodiimide chemistry. The optimal protocol employed Jeffamine/carbodiimide tissue amination, followed by reaction with activated heparin, which yielded incorporation of significant amounts of heparin within the ETVGs (about 10% heparin by tissue weight). Results also showed that PGG did not interfere with the heparinization reaction and that collagen was effectively crosslinked as evidenced by increased denaturation temperatures. Resistance to enzymatic degradation further confirmed that PGG stabilized elastin by reducing its susceptibility by almost 50%. This effect was demonstrated earlier by us for grafts derived from carotid arteries [21]. Heparinization stabilized and crosslinked collagen and increased its resistance to collagenase by 3–4 fold. Using these two selective stabilization techniques, we generated 4 main scaffold groups which were selected for implantation as direct transposition grafts in the abdominal aorta of rats and analyzed after 4 and 8 weeks: untreated, PGG-treated (elastin stabilized), heparinized (collagen stabilized) and PGG, heparin treated (elastin and collagen stabilized). Initial studies showed that the scaffolds exhibited good handling properties and were easy to implant. Survival was above 85% reaching 100% in some groups and overall patency at explantation was close to 100% in all groups.

Samples were analyzed by histology and the findings of this study could be separated into two categories; those which were unrelated to the implant treatment and those specific to the implant.

In the first category, one major finding was encapsulation of the grafts in a concentric, peri-graft vascularized granulation tissue which integrated well with the scaffold adventitia but not the media. The newly formed collagenous tissue stabilized at about 800 μm thickness after a few weeks and did not grow in thickness with time. It is known from previous work by Campbell et al. that implantation of solid objects (rods, tubes) into the peritoneal cavity or pleural cavity induces activation of macrophages and initiation of a foreign body response [30,31]. Infiltrating cells differentiate into myofibroblasts which generate a new connective tissue capsule rich in collagen surrounding the implant. These collagen tubes were later used as vascular grafts with promising results [30,31]. A similar approach was used to manufacture heart valves by implanting tricuspid valve-shaped molds subdermally in rabbits and detaching the collagenous capsule tissue [32]. In pilot studies, we also observed that essentially the same type of capsule is formed when ETVGs are implanted as direct vascular grafts in the femoral artery in minipigs (data not shown); thus it appears that this encapsulation reaction is non-specific and could beneficial after implantation of tubular grafts. Notably, porcine ETVGs did not elicit an immune reaction after implantation in rats, strengthening

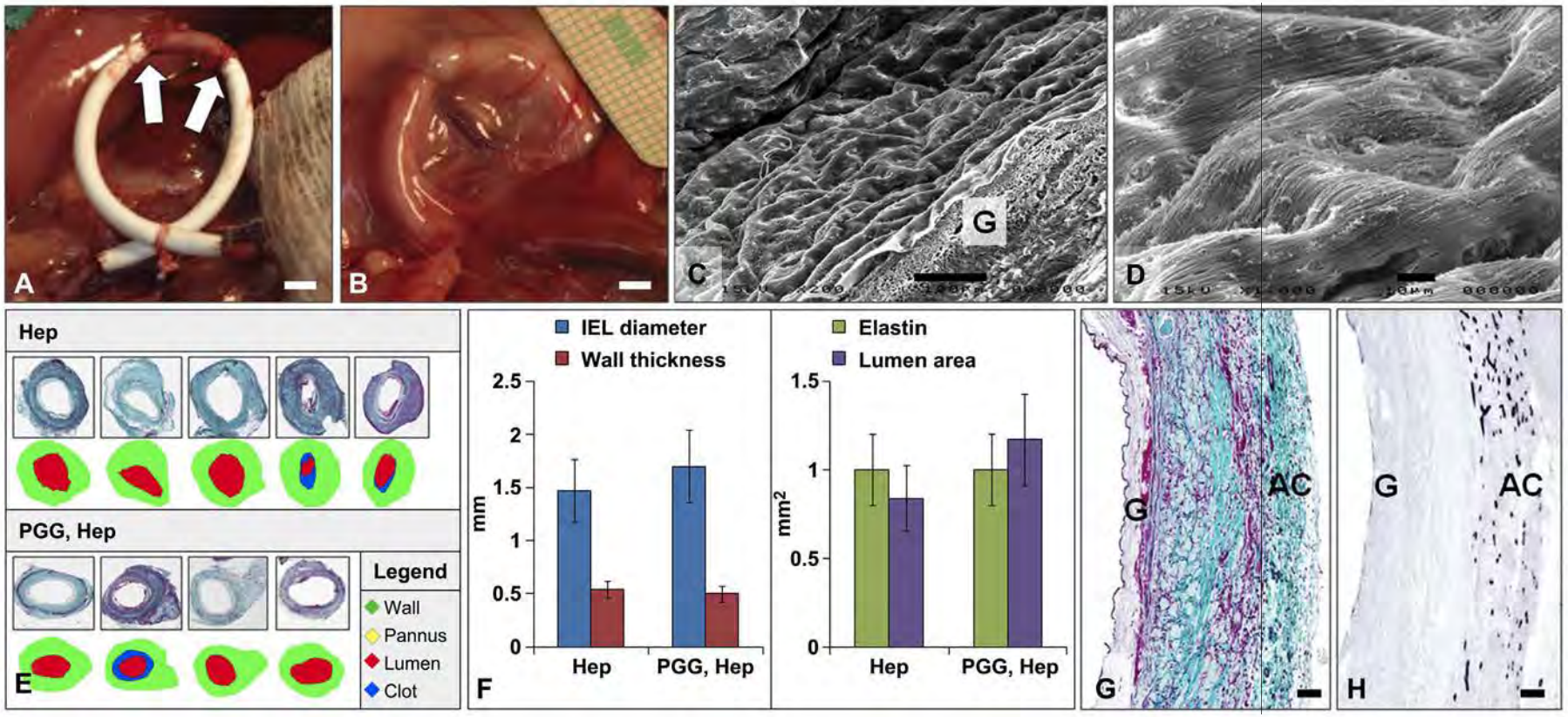

Fig. 7. Indirect isolation-loop graft evaluation. (A) Macroscopic image of indirect graft during implantation in between two ePTFE looped segments (white) and (B) at explantation. Bar is 3 mm. (C, D) SEM analysis of the scaffold lumen surface after 12 weeks implantation. G, cross section of the graft. Bar is 100 μm in (C) and 10 μm in (D). (E) Panel of representative Masson's stained mid-graft histology cross-sections from each individual implant and ETVG group: Heparin treated (Hep) and PGG followed by Heparin (PGG, Hep). Histology images were digitized and color coded to measure wall thickness (green), pannus area (yellow), lumen area (red) and clot (blue). Stained sections are shown on top and corresponding digitized images below them. (F) Quantitative morphometric data obtained from the indirect implants. Groups were: Heparin treated (Hep) and PGG followed by Heparin (PGG, Hep) treated ETVGs. IEL diameter, wall thickness, elastin and lumen area are shown. Representative images of (G) Masson trichrome stain and (H) CD31 stain for blood vessels; bar is 50 μm. AC, adventitial capsule; G, initial graft. Lumen is at left in both images. (For interpretation of the references to color in this figure legend, the reader is referred to the web version of this article.)

the hypothesis that xenogeneic matrices, if well decellularized, can serve as excellent tissue scaffolds [33,34].

Graft encapsulation occurred irrespective of the graft pre-treatment, indicating that stabilization of collagen and elastin does not prevent cell infiltration in the adventitia. While the adventitia was extensively repopulated with host cells and capillaries, few cells were found within the media of the implanted grafts. The mechanisms underlying this phenomenon are not known at this point, but it is possible that the compact IEL and adventitial elastin fibers averted cell infiltration from the lumen and adventitial sides, respectively.

Another major finding was the omnipresence of neo-intimal tissue which grew in thickness with time, remodeled and in some instances calcified. The neo-intima, potentially derived from trans-anastomotic tissue overgrowth [15,35] was covered by endothelium and thus was non-thrombogenic if intact; however, in few cases the neo-intimal tissue appeared disturbed, activated and associated with local thrombi. In all samples analyzed calcification was absent from the scaffold graft wall, denoting the fact that decellularized arteries are less prone to calcification in this model.

Several aspects were noted to depend on the scaffold pre-treatment. Only non-stabilized grafts exhibited dilatation, associated with visible elastin degeneration in vivo, specifically the IEL and the adventitial elastin fibers. PGG treatment as well as the heparinization crosslinking procedure both reduced elastin degeneration and the combination of the two was very effective in maintaining matrix integrity, pointing to stabilized arterial scaffolds as viable small diameter vascular grafts.

Overall, this is an accepted screening model for vascular grafts with the caveat that the grafts were relatively short and thus were most likely endothelialized intra-luminally by trans-anastomotic tissue overgrowth. Because of this phenomenon, it was difficult to assess the intrinsic thrombogenicity of the graft material; thus we pursued a second set of implants where the trans-anastomotic tissue overgrowth was avoided by separating the grafts from the anastomoses by two low porosity ePTFE segments (isolation-loop model or indirect grafts) with follow-up at 12 weeks as described recently [15,35]. When compared to the direct grafts these were covered by same collagenous vascularized tissue. However, by contradistinction to direct implants, the indirect grafts lacked neo-intimal tissue overgrowth with absence of thrombi. These results highlight the fact that the exposed sub-endothelial basement membrane of acellular arteries (derived from removal of the endothelium during decellularization) was essentially non-thrombogenic in this animal model.

All together, these results provide data which allow us to speculate on the outcome of clinically applicable lengths of stabilized arterial grafts as viable small diameter vascular grafts. Since in most clinical applications, segments of at least 8–10 cm long would be implanted, we expect the proximal and distal peri-anastomotic regions of the ETVGs to behave similar to the direct implants described in this paper and the midway section of the graft, at least 3–4 cm away from the anastomosis, to behave similar to the indirect implants. Currently we are testing >10 cm-long, chemically stabilized small diameter ETVGs in sheep as carotid interposition grafts.

Finally, we recommend that the optimal approach to pre-clinical testing of potential materials to be used as small diameter vascular grafts should include the following steps. If the material is biologically derived, one should first perform adequate quality controls to ensure complete decellularization as well as preservation of the major extracellular matrix components, including DNA analysis, extensive histology and α-Gal analysis. Biologic or synthetic materials of about 2.5 mm in diameter and 10 mm length could be then tested by: 1) evaluating mechanical properties, including suture retention strength, burst pressure and compliance, 2) implanting samples subdermally in rats for initial biocompatibility, as described before [21], 3) testing tubular grafts as direct vascular graft implants to evaluate peri-anastomotic reactions, 4) testing as indirect isolation-loop implants to asses host reactions away from the anastomosis and 5) implant as >10 cm long grafts in large animals for pre-clinical validation.

5. Conclusions

In the current study, we show that gentle decellularization of porcine muscular arteries generated implantable non-immunogenic small diameter ETVGs endowed with adequate mechanical properties and lack of susceptibility towards calcification. To increase stability in vivo, we chemically treated the elastin component with PGG and the collagen component with carbodiimide/heparin. Implantation of ETVGs as vascular grafts in rats resulted in high patency and animal survival, possibly due to the ubiquitous encapsulation of the grafts within a stable vascularized collagenous capsule and to the lack of thrombogenicity of the exposed sub-endothelial basement membrane. Peri-anastomotic neo-intimal tissue overgrowth was a normal occurrence in direct implants; however this reaction was circumvented in indirect, isolation-loop implants. Implantation of non-stabilized ETVGs exhibited marked graft dilatation and elastin degeneration; however chemical stabilization of grafts significantly reduced elastin degradation and prevented aneurismal dilatation of vascular grafts in vivo without altering formation of the external capsule. Due to their resistance to thrombosis, dilatation and calcification, stabilized acellular arteries are promising candidates as small diameter vascular grafts.

Disclosure statement

The authors have no competing financial interests.

Acknowledgments

The authors wish to acknowledge the excellent technical support of Helen Ilsley and Anel Oosthuysen from UCT and the NIH Fogarty International Research Collaboration Research Award (FIRCA, R03 TW008941) to DS.

References

[1] Faries PL, Logerfo FW, Arora S, Pulling MC, Rohan DI, Akbari CM, et al. Arm vein conduit is superior to composite prosthetic-autogenous grafts in lower extremity revascularization. J Vasc Surg 2000;31:1119–27.
[2] Farber A, Major K, Wagner WH, Cohen JL, Cossman DV, Lauterbach SR, et al. Cryopreserved saphenous vein allografts in infrainguinal revascularization: analysis of 240 grafts. J Vasc Surg 2003;38:15–21.
[3] Zehr BP, Niblick CJ, Downey H, Ladowski JS. Limb salvage with CryoVein cadaver saphenous vein allografts used for peripheral arterial bypass: role of blood compatibility. Ann Vasc Surg 2011;25:177–81.
[4] Brewster DC. Current controversies in the management of aortoiliac occlusive disease. J Vasc Surg 1997;25:365–79.
[5] Klinkert P, Post PN, Breslau PJ, van Bockel JH. Saphenous vein versus PTFE for above-knee femoropopliteal bypass. A review of the literature. Eur J Vasc Endovasc Surg 2004;27:357–62.
[6] Kurobe H, Maxfield MW, Breuer CK, Shinoka T. Concise review: tissue-engineered vascular grafts for cardiac surgery: past, present, and future. Stem Cells Transl Med 2012;1:566–71.
[7] Huang AH, Niklason LE. Engineering of arteries in vitro. Cell Mol Life Sci; 2014. http://dx.doi.org/10.1007/s00018-013-1546-3.
[8] Klopsch C, Steinhoff G. Tissue-engineered devices in cardiovascular surgery. Eur Surg Res 2012;49:44–52.
[9] Cleary MA, Geiger E, Grady C, Best C, Naito Y, Breuer C. Vascular tissue engineering: the next generation. Trends Mol Med 2012;18:394–404.
[10] Chow JP, Simionescu DT, Warner H, Wang B, Patnaik SS, Liao J, et al. Mitigation of diabetes-related complications in implanted collagen and elastin scaffolds using matrix-binding polyphenol. Biomaterials 2013;34:685–95.

[11] Tedder ME, Liao J, Weed B, Stabler C, Zhang H, Simionescu A, et al. Stabilized collagen scaffolds for heart valve tissue engineering. Tissue Eng A 2009;15:1257–68.
[12] Isenburg JC, Simionescu DT, Vyavahare NR. Elastin stabilization in cardiovascular implants: improved resistance to enzymatic degradation by treatment with tannic acid. Biomaterials 2004;25:3293–302.
[13] Simionescu DT, Lu Q, Song Y, Lee JS, Rosenbalm TN, Kelley C, et al. Biocompatibility and remodeling potential of pure arterial elastin and collagen scaffolds. Biomaterials 2006;27:702–13.
[14] Lu Q, Ganesan K, Simionescu DT, Vyavahare NR. Novel porous aortic elastin and collagen scaffolds for tissue engineering. Biomaterials 2004;25:5227–37.
[15] Pennel T, Zilla P, Bezuidenhout D. Differentiating transmural from transanastomotic prosthetic graft endothelialization through an isolation loop-graft model. J Vasc Surg 2013;58:1053–61.
[16] Tai NRM, Giudiceandrea A, Salacinski HJ, Seifalian AM, Hamilton G. In vivo femoropopliteal arterial wall compliance in subjects with and without lower limb vascular disease. J Vasc Surg 1999;30:936–45.
[17] Riesenfeld J, Roden L. Quantitative analysis of N-sulfated, N-acetylated, and unsubstituted glucosamine amino groups in heparin and related polysaccharides. Anal Biochem 1990;188:383–9.
[18] Bezuidenhout D, Davies N, Black M, Schmidt C, Oosthuysen A, Zilla P. Covalent surface heparinization potentiates porous polyurethane scaffold vascularization. J Biomater Appl 2010;24:401–18.
[19] Bezuidenhout D, Oosthuysen A, Human P, Weissenstein C, Zilla P. The effects of cross-link density and chemistry on the calcification potential of diamine-extended glutaraldehyde-fixed bioprosthetic heart-valve materials. Biotechnol Appl Biochem 2009;54:133–40.
[20] Beckstead JH. A simple technique for preservation of fixation-sensitive antigens in paraffin-embedded tissues. J Histochem Cytochem 1994;42:1127–34.
[21] Chuang TH, Stabler C, Simionescu A, Simionescu DT. Polyphenol-stabilized tubular elastin scaffolds for tissue engineered vascular grafts. Tissue Eng A 2009;15:2837–51.
[22] Mercuri JJ, Patnaik S, Dion G, Gill SS, Liao J, Simionescu DT. Regenerative potential of decellularized porcine nucleus pulposus hydrogel scaffolds: stem cell differentiation, matrix remodeling, and biocompatibility studies. Tissue Eng A 2013;19:952–66.
[23] Wu W, Allen R, Gao J, Wang YD. Artificial niche combining elastomeric substrate and platelets guides vascular differentiation of bone marrow mononuclear cells. Tissue Eng A 2011;17:1979–92.
[24] Brennan MP, Dardik A, Hibino N, Roh JD, Nelson GN, Papademitris X, et al. Tissue-engineered vascular grafts demonstrate evidence of growth and development when implanted in a juvenile animal model. Ann Surg 2008;248:370–7.
[25] Naito Y, Williams-Fritze M, Duncan DR, Church SN, Hibino N, Madri JA, et al. Characterization of the natural history of extracellular matrix production in tissue-engineered vascular grafts during neovessel formation. Cells Tissues Organs 2012;195:60–72.
[26] Isenburg JC, Karamchandani NV, Simionescu DT, Vyavahare NR. Structural requirements for stabilization of vascular elastin by polyphenolic tannins. Biomaterials 2006;27:3645–51.
[27] Isenburg JC, Simionescu DT, Starcher BC, Vyavahare NR. Elastin stabilization for treatment of abdominal aortic aneurysms. Circulation 2007;115:1729–37.
[28] Zhang J, Li L, Kim SH, Hagerman AE, Lu J. Anti-cancer, anti-diabetic and other pharmacologic and biological activities of penta-galloyl-glucose. Pharm Res 2009;26:2066–80.
[29] Sierad LN, Simionescu A, Albers C, Chen J, Maivelett J, Tedder ME, et al. Design and testing of a pulsatile conditioning system for dynamic endothelialization of polyphenol-stabilized tissue engineered heart valves. Cardiovasc Eng Technol 2010;1:138–53.
[30] Chue WL, Campbell GR, Caplice N, Muhammed A, Berry CL, Thomas AC, et al. Dog peritoneal and pleural cavities as bioreactors to grow autologous vascular grafts. J Vasc Surg 2004;39:859–67.
[31] Campbell JH, Efendy JL, Campbell GR. Novel vascular graft grown within recipient's own peritoneal cavity. Circ Res 1999;85:1173–8.
[32] Hayashida K, Kanda K, Yaku H, Ando J, Nakayama Y. Development of an in vivo tissue-engineered, autologous heart valve (the biovalve): preparation of a prototype model. J Thorac Cardiovasc Surg 2007;134:152–9.
[33] Crapo PM, Gilbert TW, Badylak SF. An overview of tissue and whole organ decellularization processes. Biomaterials 2011;32:3233–43.
[34] Badylak SF, Freytes DO, Gilbert TW. Extracellular matrix as a biological scaffold material: structure and function. Acta Biomater 2009;5:1–13.
[35] Zilla P, Bezuidenhout D, Human P. Prosthetic vascular grafts: wrong models, wrong questions and no healing. Biomaterials 2007;28:5009–27.